

RADIO-LOUD NARROW-LINE TYPE 1 QUASARS

STEFANIE KOMOSSA AND WOLFGANG VOGES

Max-Planck-Institut für Extraterrestrische Physik, Postfach 1312, 85741 Garching, Germany; skomossa@mpe.mpg.de

DAWEI XU

National Astronomical Observatories, Chinese Academy of Sciences, A20 Datun Road, Chaoyang District, Beijing 100012, China

SMITA MATHUR

Department of Astronomy, The Ohio State University, 140 West 18th Avenue, Columbus, OH 43210

HANS-MARTIN ADORF

Max-Planck-Institut für Extraterrestrische Physik, Postfach 1312, 85741 Garching, Germany; and Max-Planck-Institut für Astrophysik, Karl-Schwarzschild-Strasse 1, 85748 Garching, Germany

GERARD LEMSON

Max-Planck-Institut für Extraterrestrische Physik, Postfach 1312, 85741 Garching, Germany

WOLFGANG J. DUSCHL

Institut für Theoretische Astrophysik, Albert-Ueberle-Strasse 2, 69120 Heidelberg Germany; and Steward Observatory, The University of Arizona, 933 North Cherry Avenue, Tucson, AZ 85721

AND

DIRK GRUPE

Astronomy Department, Pennsylvania State University, 525 Davey Laboratory, University Park, PA 16802

Received 2005 December 19; accepted 2006 April 11

ABSTRACT

We present the first systematic study of (non-radio-selected) radio-loud narrow-line Seyfert 1 (NLS1) galaxies. Cross-correlation of the Catalogue of Quasars and Active Nuclei with several radio and optical catalogs led to the identification of ~ 11 radio-loud NLS1 candidates, including four previously known ones. This study almost triples the number of known radio-loud NLS1 galaxies if all candidates are confirmed. Most of the radio-loud NLS1 galaxies are compact, steep-spectrum sources accreting close to or above the Eddington limit. The radio-loud NLS1 galaxies of our sample are remarkable in that they occupy a previously rarely populated regime in NLS1 multiwavelength parameter space. While their $[\text{O III}]/\text{H}\beta$ and $\text{Fe II}/\text{H}\beta$ intensity ratios almost cover the whole range observed in NLS1 galaxies, their radio properties extend the range of radio-loud objects to those with small widths of the broad Balmer lines. Their black hole masses are generally at the upper observed end among NLS1 galaxies but are still unusually small in view of the radio loudness of the sources. Among the radio-detected NLS1 galaxies, the radio index R is distributed quite smoothly up to the critical value of $R \simeq 10$ and covers about 4 orders of magnitude in total. Statistics show that $\sim 7\%$ of the NLS1 galaxies are formally radio-loud, while only 2.5% exceed a radio index $R > 100$. Implications for NLS1 models are discussed. Several mechanisms are considered as explanations for the radio loudness of the NLS1 galaxies and for the lower frequency of radio-loud galaxies among NLS1 galaxies than among quasars. While properties of most sources (with two to three exceptions) generally do not favor relativistic beaming, the combination of accretion mode and spin may explain the observations.

Key words: quasars: emission lines — quasars: general — quasars: individual (TEX 1111+329, SDSS J094857.3+002225, SDSS J172206.03+565451.6, RX J0134–4258, IRAS 09426+1929, SBS 1517+520, RX J16290+4007, PKS 0558–504, 2E 1346+2637, IRAS 20181–2244, RX J23149+2243) — radio continuum: galaxies — X-rays: galaxies

1. INTRODUCTION

The radio-loud/radio-quiet bimodality of quasars is one of the long-standing unsolved problems in the research of active galactic nuclei (AGNs). While the presence of two classes of quasars, radio-loud and radio-quiet, with a deficiency of sources at intermediate radio power, has been historically apparently well established (e.g., Kellerman et al. 1989; Miller et al. 1990; Visnovsky et al. 1992), other studies have questioned the mere existence of a radio dichotomy (e.g., White et al. 2000; Cirasuolo et al. 2003) or have pointed out that larger samples are needed to put the bimodality on a firmer statistical basis (Hooper et al. 1995). On the other hand, it has been argued that carefully selected, small, well-studied samples still reveal the bimodality (e.g., Sulentic et al.

2003) and that it is still present in a large sample of Sloan Digital Sky Survey (SDSS)/Faint Images of the Radio Sky at Twenty cm (FIRST) galaxies (Ivezić et al. 2002). Approximately 15% of the quasar population is radio-loud (Urry & Padovani 1995) for reasons that are still unknown.

A second question that is currently under close scrutiny is whether or not there are relations between black hole mass and radio loudness, and especially whether or not there is a limiting black hole mass above which objects are preferentially radio-loud, and whether or not radio-loud and radio-quiet galaxies show the same spread in their black hole masses (e.g., Laor 2000; Lacy et al. 2001; Oshlack et al. 2002; Woo & Urry 2002; Shields et al. 2003; McLure & Jarvis 2004; Metcalf & Magliocchetti 2006; Liu et al. 2006).

While most attention has so far concentrated on the radio-loud/radio-quiet distinction of quasars, extending the studies to other subtypes of AGNs may shed new light both on the existence of the radio-loud/radio-quiet bimodality and on the cause of radio loudness. We have started an investigation of the radio properties of narrow-line Seyfert 1 (NLS1) galaxies. Apart from the topic just mentioned, the analysis of their radio properties is also of interest for addressing open questions in the study of NLS1 galaxies, as detailed below.

NLS1 galaxies were identified by Osterbrock & Pogge (1985) as objects with small widths of the broad Balmer lines. These go hand-in-hand with weak [O III] $\lambda 5007/H\beta_{\text{tot}}$ emission and strong emission from Fe II complexes (e.g., Boroson & Green 1992). Physical drivers of the NLS1 phenomenon and correlations among emission-line and continuum properties are not yet well understood. There is growing evidence, however, that most NLS1 galaxies are objects with high accretion rates, close to or even above the Eddington rate, and low black hole masses (e.g., Boroson & Green 1992; Pounds et al. 1995; Wang et al. 1996; Boller et al. 1996; Laor et al. 1997; Czerny et al. 1997; Marziani et al. 2001; Boroson 2002; Simkin & Roychowdhury 2003; Xu et al. 2003; Kawaguchi 2003; Wang & Netzer 2003; Grupe 2004; Grupe & Mathur 2004; Botte et al. 2004; Collin & Kawaguchi 2004). Apart from that, several other parameters have been suggested to influence the main properties of NLS1 galaxies, including orientation (e.g., Osterbrock & Pogge 1985; Bian & Zhao 2004), winds and density effects (e.g., Lawrence et al. 1997; Wills et al. 2000; Bachev et al. 2004; Xu et al. 2003, 2006), metallicity (e.g., Mathur 2000; Komossa & Mathur 2001; Shemmer & Netzer 2002; Nagao et al. 2002; Warner et al. 2004; Fields et al. 2005), and absorption (e.g., Komossa & Meerschweinchen 2000; Gierlinski & Done 2004). There is evidence that NLS1 galaxies follow a different black hole mass–velocity dispersion ($M_{\text{BH}}-\sigma$) relation from that for broad-line Seyfert 1 galaxies (e.g., Mathur 2001; Grupe & Mathur 2004; Mathur & Grupe 2005), with important implications for galaxy evolution and black hole growth.

While the X-ray and optical properties of NLS1 galaxies have been explored intensively in the last decade, relatively little is known about their radio properties. Ulvestad et al. (1995) observed seven NLS1 galaxies with the Very Large Array (VLA) and concluded that they are only of modest radio power and that the radio emission is more compact than a few hundred parsecs. Moran (2000) studied 24 NLS1 galaxies with the VLA and found that most of the sources are unresolved and show relatively steep spectra. Stepanian et al. (2003) found nine radio-detected (FIRST) NLS1 galaxies among 26 NLS1 galaxies of the Second Byurakan Survey, all of them radio-quiet. Greene et al. (2006) performed radio observations of 19 galaxies with low black hole masses, several of them with optical spectra similar to NLS1 galaxies. They only detected one source.

So far, only a few radio-loud NLS1 galaxies have been identified.¹ PKS 0558–504 (Remillard et al. 1986; Siebert et al. 1999), RX J0134–4258 (Grupe et al. 2000), SDSS J094857.3+002225 (Zhou et al. 2003), and SDSS J172206.03+565451.6 (Komossa et al. 2006) all exceed radio indices $R = 10$ and show optical NLS1 spectra. RGB J0044+193 (Siebert et al. 1999) is radio-quiet most of the time (Maccarone et al. 2005) but may have been radio-loud at the epoch of the Green Bank Radio Survey (87GB; Siebert et al. 1999; Maccarone et al. 2005) due to variability in the radio band. PKS 2004–447 (Oshlack et al. 2001) is a (nontypical)

NLS1 or possibly a narrow-line radio galaxy (Zhou et al. 2003) and is very radio-loud.

It is still a puzzle why radio-loud NLS1 galaxies are scarce. In particular, it is still unclear whether they are truly preferentially radio-quiet, or rather that the scarcity of radio-loud galaxies is due to some selection effect. This question can be addressed by a systematic search for, and study of, radio-loud NLS1 galaxies.

The study of radio properties of NLS1 galaxies, in particular their radio loudness and radio variability, also allows us to re-address the question of whether NLS1 galaxies are preferentially viewed face-on. Furthermore, radio observations of NLS1 galaxies provide constraints on the coupling between jets and accretion disks (e.g., Zdziarski et al. 2003). There are indications that objects with accretion rates close to the Eddington rate tend to be radio-weaker; a behavior observed in Galactic X-ray binaries in the soft/high state and AGNs (Maccarone et al. 2003; Greene et al. 2006; and references therein).

Here we report results from a search for radio-loud and “almost radio-loud” NLS1 galaxies, based on cross-correlating a catalog of optically identified NLS1 galaxies with radio catalogs. This is the first systematic study of (non-radio-selected) radio-loud NLS1 galaxies and of their radio, optical, and X-ray properties. We use the term “NLS1 galaxy” collectively for high-luminosity and low-luminosity objects, i.e., for narrow-line type 1 quasars and for narrow-line Seyfert type 1 galaxies. A cosmology with $H_0 = 70 \text{ km s}^{-1} \text{ Mpc}^{-1}$, $\Omega_M = 0.3$, and $\Omega_\Lambda = 0.7$ is adopted throughout this paper.

This paper is organized as follows: In § 2 we describe our methods for cross-matching a large number of catalogs and present candidate radio-loud NLS1 galaxies. In §§ 3 and 4 we provide results from our analysis of the optical and X-ray spectra of these NLS1 galaxies. Consequences of our results for NLS1 models, and mechanisms to explain the lower frequency of radio-loud galaxies among NLS1 galaxies than among quasars are discussed in § 5.

2. GERMAN ASTROPHYSICAL VIRTUAL OBSERVATORY SEARCH FOR RADIO-LOUD NLS1 GALAXIES

2.1. Search Methods

In order to search for radio-loud NLS1 galaxies and study their properties, we extracted all NLS1 galaxies included in the 11th edition of the Catalogue of Quasars and Active Nuclei compiled by Véron-Cetty & Véron (2003, hereafter VQC03), separately for the catalog of “faint” objects (i.e., Seyfert galaxies fainter than absolute magnitude $M = 23$) and the “bright” ones (i.e., quasars brighter than $M = 23$). We present results for the narrow-line type 1 quasars here, while results for the Seyfert galaxies will be reported elsewhere. The defining criterion for inclusion as a NLS1 galaxy in the VQC03 is the width of the $H\beta$ emission line: $\text{FWHM}_{H\beta} < 2000 \text{ km s}^{-1}$. The list of the 128 selected narrow-line quasars was then cross-correlated with the FIRST (at 1.4 GHz; White et al. 1997; Becker et al. 1995), the NVSS (NRAO VLA Sky Survey, at 1.4 GHz; Condon et al. 1998), the SUMSS (Sydney University Molonglo Sky Survey, at 843 MHz; Mauch et al. 2003), the WENSS (Westerbork Northern Sky Survey, at 0.33 GHz),² the PMN (Parkes-MIT-NRAO radio survey, including the Southern Survey, Zenith Survey, Tropical Survey, and Equatorial Survey, at 4.85 GHz; Griffith et al. 1994), the 87GB (at 4.85 GHz; Gregory & Condon 1991), and the PKS (Parkes Radio Survey, at 2.7 GHz)³ radio catalogs, in order to select all radio-detected NLS1 galaxies,

¹ There are preliminary reports that optical identifications of FIRST radio sources produce a higher rate of radio-loud NLS1 galaxies than optical selection (Whalen et al. 2001; see our § 6 for a comparison with Whalen et al. 2006).

² VizieR Online Data Catalog, VIII/62 (G. de Bruyn et al., 1998).

³ VizieR Online Data Catalog, VIII/15 (A. E. Wright & R. Otrupceck, 1990).

and among these the radio-loud ones. The input list was simultaneously cross-correlated with the USNO-B1 (Monet et al. 2003), USNO-A2, and Guide Star Catalog, version 2.2 (GSC2.2), optical photometry catalogs in order to obtain blue magnitudes.

For cross-matching of radio catalogs with optical catalogs we used the cross-matcher application developed within the German Astrophysical Virtual Observatory (GAVO)⁴ project. The GAVO cross-matcher is a multiarchive, multiserver, multicatalog, statistical spatial matcher operating solely on astrometric coordinates and their uncertainties (Adorf et al. 2003, 2006).

In our case, it takes as input an extract of the VQC03 catalog, which includes all NLS1 galaxies in that catalog and their coordinates. A query module then accesses the VizieR archive⁵ and extracts coordinates and flux and magnitude data from selected catalogs in the archive.

While the VizieR match-list services are capable of deterministically matching the input list against a single catalog, we then proceed in matching the different output lists against each other in order to find the most likely single multiwavelength “counterpart.” In the first step, match candidates are generated in the following way: combinations of potential counterparts are formed, which are viewed as hypothetical “clusters” on the sky. For each such cluster its central position is computed, followed by a computation of the projected distances on the sky between each counterpart candidate and the central cluster position.

Next, based on the astrometric positions and associated uncertainties, for each counterpart in a given match candidate cluster its isotropic Mahalanobis distance (Mahalanobis 1936; Devroye et al. 1996) to the central cluster position is computed. It measures the statistical distance to the cluster center. For each cluster a goodness-of-fit criterion is computed, namely, the standard χ^2 metric, which is simply the sum of the squared Mahalanobis distances. It can be viewed as a measure of compactness of the cluster, where instead of the physical distances, the statistical distances are being used.

Since the number of counterparts contributing to a match candidate generally differs from candidate to candidate, we cannot use the χ^2 metric directly for comparing the goodness of the match. Instead, the reduced χ^2 metric is computed. For the required degrees of freedom N_f we use $N_f = 2N_i - 2$, where N_i denotes the number of counterparts contributing to a match candidate. We subtract 2 in order to allow for the estimation (“fitting”) of the two sky coordinates, i.e., right ascension and declination, when computing the cluster center. A reduced χ^2 threshold parameter is used for discriminating against unreasonable match combinations. Finally, for each remaining match candidate, the cross-matcher extracts the astrometry and optical and radio photometry data.

Either position uncertainties inherent to the different (radio) surveys are taken into account on an object-by-object basis if individual position errors are available (this is generally the case for the FIRST and 87GB catalogs in VizieR: typically $1''$ [FIRST] and $<30''$ [87GB]), or else typical average position uncertainties d for the different catalogs are used (explicitly, $d = 1''$ [USNO-A2, USNO-B1, and GSC2.2], $7''$ [NVSS], $30''$ [PKS and PMN], and $10''$ [SUMSS and WENSS]). The catalog-specific search radii were typically larger by a factor of 3.

2.2. Safety Checks and Data Screening

While this automated way of simultaneously cross-correlating various catalogs and of selecting counterparts is generally very successful, there are still a number of “peculiarities” inherent to

the way the catalogs were produced in general, or to individual galaxies in particular, that affect the cross-matching output and that make it necessary to check a number of results by hand. While the long-term goal is to include most of these effects into the cross-correlation software, in this pilot project we paid special attention to actually identifying potential problems and effects that will need closer attention in the future when applying similar cross-correlation methods to much larger samples.

Nearby bright galaxies are missed in blue magnitude catalogs because they are too extended and too bright for standard automated magnitude measurements to still work. This is not a problem for the present sample, since the quasars are sufficiently distant, but will be more severe for samples of nearby Seyfert galaxies.

A few cataloged NLS1 galaxies still have optical coordinate offsets that are larger than expected in the optical band. One reason is that their *IRAS* coordinates rather than optical coordinates were still listed, which come with a larger uncertainty. Therefore, counterparts in blue magnitudes and FIRST radio sources might be missed. For the present sample, IRAS 11598–0112 and RX J01354–0426 were not assigned optical counterparts by the original cross-correlation procedure. IRAS 11598–0112 had its *IRAS* coordinates cataloged, while the true optical coordinates then turn out to be consistent with the FIRST radio position. The optical counterpart of RX J01354–0426 is offset by $\sim 3''$ – $4''$ from the coordinate in the VQC03. However, since there is no other good multiwavelength counterpart in the field, we assume that the optical, radio, and X-ray sources are one and the same.

Bright radio sources are often detected in several surveys with widely different positional uncertainties. In that case it is generally a good idea to then use the smallest positional error among the radio catalogs for further cross-correlation with nonradio catalogs to reduce the number of potential multiwavelength match candidates. In the present study, in two cases, a bright source was detected in several radio surveys, suggesting that we were dealing with one and the same source, but the source coordinates in those radio surveys with small coordinate uncertainties were no longer consistent with the optical position. In the specific case of RX J07101+5002, only a 87GB counterpart was found by cross-correlation, $45''$ off the optical position. The 87GB source has counterparts in several other radio catalogs, including NVSS and FIRST, which show the same offset from the optical coordinates and similar radio fluxes. This means the radio source is one and the same in all radio catalogs. However, given the small coordinate uncertainty in the FIRST catalog, it can no longer be related to the optical NLS1 galaxy. The FIRST image reveals a complex radio structure with several bright knots and lobes. We have checked that none of these substructures coincides with the optical NLS1. Rather, the core of the radio galaxy does have a “normal” galaxy as an optical counterpart, reported by Bauer et al. (2000). The question remains whether the *X-ray source* RX J07101+5002 is then actually the counterpart to the radio source (as often assumed; e.g., Bauer et al. 2000), or whether it is the counterpart to the optical NLS1 galaxy, as concluded by Xu et al. (2003), who provided the optical spectroscopy of that source. The radio galaxy is radio-loud, with $R_{1.4} = 64$. We exclude it from the sample, however, since the NLS1 galaxy is not its counterpart. In the case of SBS 1330+519, only a WENSS counterpart was found, offset by $20''$. The WENSS source has FIRST and NVSS counterparts that, however, are too far off from the optical position of SBS 1330+519 to still be considered as counterparts. SBS 1330+519 was thus excluded from our sample. We note in passing that the relatively strong radio source itself does have a very faint optical counterpart in the SDSS (York et al. 2000) photometric catalog (Abazajian et al. 2005), SDSS

⁴ See <http://www.g-vo.org>.

⁵ See <http://vizier.u-strasbg.fr/viz-bin/VizieR>.

J133219.38+514439.9. With SDSS r and g magnitudes of 21.5 and 22.3 mag, respectively, this background object is very radio-loud ($R_{1.4} = 8940$). No optical spectrum is available.

Radio images of all radio-detected NLS1 galaxies were inspected by eye to convince ourselves of the reliability of counterpart identification.

2.3. Assessment of Radio Loudness

For all confirmed radio-detected objects, their radio loudness was then estimated following Kellermann et al. (1989), who define the radio index R as the ratio of the 6 cm radio flux to the optical flux at 4400 Å. The value $R = 10$ is commonly used to mark the “border” between radio-quiet and radio-loud objects, originally calculated based on the assumption of similar spectral shapes in the optical and radio band with $\alpha = -0.5$ (Kellermann et al. 1989). The radio surveys employed in the present study generally measure at 1.4 GHz. Still keeping the same assumptions, in particular $\alpha = -0.5$, we compute the radio index at 1.4 GHz as $R_{1.4} = 1.9R$, and we use $R_{1.4} = 19$ as a reasonable distinction between radio-loud and radio-quiet objects. Optical blue magnitudes m_{B2} were extracted from the USNO-B1 catalog and used to calculate $R_{1.4}$. For comparison, blue magnitudes from the first epoch of the USNO-B1 (m_{B1}), the GSC2.2 (m_B), and the USNO-A2 (m_B) catalogs were also collected to get an impression of the uncertainty in blue magnitude, which would be due to either source-intrinsic variability or measurement uncertainties.

As a last step, only a careful object-by-object check can tell which objects were actually radio-loud NLS1 galaxies, or good candidates. In particular, peculiar intrinsic spectral shapes, high redshift, or heavy absorption, which affect the radio and optical bands in different ways, would invalidate the simple way of calculating the radio index R as the ratio of *observed* radio to optical flux density. Also, merging galaxies with close double nuclei make counterpart identification ambiguous. Finally, optical spectroscopic classification of each radio-loud candidate needs to be checked carefully in order to confirm its NLS1 nature. An uncertainty that generally cannot be overcome with existing data given their nonsimultaneity is source variability in either the optical or radio band.

2.4. Search Results

2.4.1. General Results

Among the 128 NLS1 galaxies in the VQC03 we find that 35 have radio counterparts in one or more catalogs. In Figure 1 we present the distribution of their radio indices $R_{1.4}$. Formally, among this sample ~ 11 objects exceed or are close to the “critical” value of $R_{1.4} = 19$ commonly used to distinguish between radio-quiet and radio-loud objects. The radio-loud NLS1 galaxies are TEX 11111+329, SDSS J094857.3+002225, SDSS J172206.03+565451.6, IRAS 20181–2244, RX J0134–4258, PKS 0558–504, IRAS 09426+1929, SBS 1517+520, RX J16290+4007, 2E 1346+2637, and RX J23149+2243 (Table 1; sources are listed by their name as given in the VQC03). Among these, we recover the previously known radio-loud NLS1 galaxies PKS 0558–504, RX J0134–4258, SDSS J172206.03+565451.6, and SDSS J094857.3+002225.⁶ PKS 2004–447, not included in our sam-

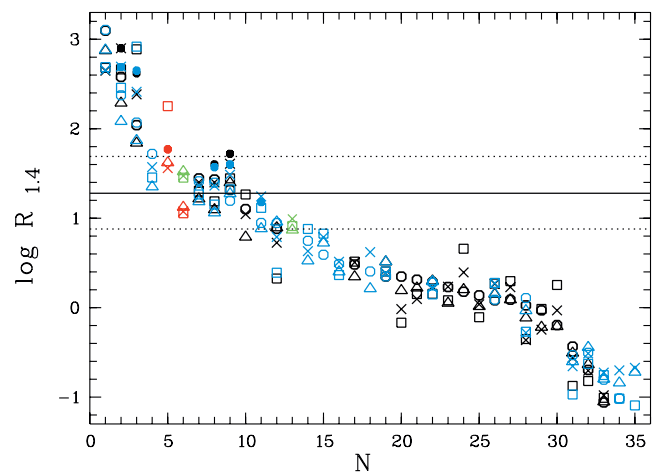


FIG. 1.—Radio-detected NLS1 galaxies selected from the VQC03, ordered according to radio loudness. The solid line marks the dividing line between radio-loud and radio-quiet objects, $R_{1.4} = 19$ (corresponding to $R = 10$; see text for definitions). Calculation of $R_{1.4}$ is generally based on USNO-B1 blue magnitudes m_{B2} (squares) and FIRST (black) and/or NVSS (blue) radio detections, except for RX J0134–4258 (PMN data at 4.85 GHz, red), PKS 0558–504 (PMN data, red; SUMSS data at 0.8 GHz, green), and RX J22179–5941 (SUMSS data, green). Several FIRST/NVSS objects have radio detections at other wavelengths. These are not overplotted here but are used for estimates of radio spectral indices (Table 1). In order to have an estimate of the uncertainty in m_B —due to either real source variability or measurement uncertainties—we also show $R_{1.4}$ calculated using m_{B1} (circles) of the USNO-B1 catalog, m_B of the USNO-A2 catalog (triangles), m_B , taken from GSC2.2 (crosses), and corrected 4400 Å fluxes obtained from the SDSS, ESO, and Xinglong spectra (small filled circles). The dotted line indicates a change in blue magnitude by $\Delta m_B = \pm 1$ mag. Plotted ratios are for the following galaxies, from left to right: ($N=1$) TEX 11111+329, (2) SDSS J094857.3+002225, (3) SDSS J172206.03+565451.6, (4) IRAS 20181–2244, (5) RX J0134–4258, (6) PKS 0558–504, (7) IRAS 09426+1929, (8) SBS 1517+520, (9) RX J16290+4007, (10) 2E 1346+2637, (11) RX J23149+2243, (12) IRAS 11598–0112, (13) RX J22179–5941, (14) IRAS 00275–2859, (15) IRAS 20520–2329, (16) RX J01354–0426, (17) MS 12510–0031, (18) IRAS 11058+7159, (19) HS 0710+3825, (20) SBS 1152+523, (21) SBS 1126+516, (22) IRAS 13349+2438, (23) RX J15308+2026, (24) RX J16196+2543, (25) RX J11425+2503, (26) RX J15475+1024, (27) FBS 1002+437, (28) PG 1404+226, (29) RX J17025+3247, (30) RX J12257+2055, (31) PG 1448+273, (32) Mrk 478, (33) PHL 1811, (34) 1Zw 1, (35) IRAS 13224–3809.

ple since it is a Seyfert galaxy rather than a quasar, is unusual in almost lacking Fe II emission in its optical spectrum (Oshlack et al. 2001), which led to the suggestion it could be a narrow-line radio galaxy or a type 2 AGN. Given the large scatter in Fe II of the radio-loud objects of our sample, it is very possible that PKS 2004–447 is similar, just at the low Fe II end, and we include it in Table 1.

Based on average blue magnitudes of the nondetected sources and given the NVSS flux limit (~ 2.5 mJy), no more very radio-loud sources are expected among the nondetections. Several more borderline objects close to $R_{1.4} \approx 19$ could exist, but only if their radio flux was just exactly below the NVSS flux limit.

Radio source positions agree well with the optical coordinates of the sources. FIRST counterpart position offsets are typically $< 1''$, while NVSS offsets are typically $< 5''$. The radio emission of the radio-loud NLS1 galaxies is generally compact. Their FIRST extent is always $< 2''$, which is consistent with point sources (White et al. 1997).

The 35 radio-detected sources cover about 4 orders of magnitude in radio index R . Below $\log R \approx 1$ (Fig. 1) the data hint at a rather smooth distribution of radio indices, while only a few objects are well above $\log R \approx 1$. In this small sample, data do not cluster at certain R -values, and only some weak hints for a bimodal distribution appear (Fig. 2). A number of our objects

⁶ Wang et al. (2004) claimed the detection of another radio-loud NLS1 galaxy, SDSS J022119.8+005628.4. However, the position offset between the SDSS galaxy and the faint NVSS radio source is $24''$, much larger than the expected offset of $\sim 7''$ for faint sources. Furthermore, we do not find any radio counterpart in the FIRST survey, indicating that the very faint NVSS counterpart, if real, is either very extended or variable. Deeper radio observations are needed to confirm the existence of this radio source and to see whether it is indeed the counterpart to the NLS1 galaxy.

TABLE 1
SUMMARY OF THE RADIO PROPERTIES OF RADIO-LOUD NLS1 GALAXIES AND CANDIDATES

Name	z	R	ν_R (GHz)	α_r	ν_1 (GHz)	ν_2 (GHz)	Comments
TEX 11111+329.....	0.189	1249–445	1.4	–0.56 –1.24 <–2.07	0.33 1.4 1.4	1.4 4.85 15	Optically absorbed Upper limit at 15 GHz (Nagar et al. 2003)
SDSS J094857+002225.....	0.584	793–194 >1000	1.4 5	0.59	2.7	4.85	Variable (Zhou et al. 2003)
SDSS J172206+565451.....	0.425	773–70	1.4	–0.69	0.33	1.4	Komossa et al. (2006)
RX J0134–4258.....	0.237	178–36	4.85	–1.43	4.85	8.4	See also Grupe et al. (2000)
IRAS 20181–2244.....	0.185	52–22	1.4	–0.51	0.35	1.4	
RX J16290+4007.....	0.272	41–21 68–35	1.4 4.85	0.42	1.4	4.85	
IRAS 09426+1929.....	0.284	28–16	1.4				
PKS 0558–504.....	0.137	16–14	4.85	–0.45 –0.38	2.7 0.84	4.85 2.7	
RX J23149+2243.....	0.168	18–8	1.4				
2E 1346+2637.....	0.915	18–6	1.4				
SBS 1517+520.....	0.371	27–12	1.4				
PKS 2004–447.....	0.24	6320–1710	4.85	–0.67	ATCA		Variable (Oshlack et al. 2001)

NOTES.—PKS 2004–447 (a peculiar NLS1 galaxy; Oshlack et al. 2001) was added for comparison. The range in radio index R of each galaxy is defined by the choice of the blue magnitudes from different epochs/catalogs as in Fig. 1, and is based on FIRST observations if available. The z column is redshift, ν_R gives the observed frequency at which R was calculated, α_r is the radio power-law spectral index ($f_\nu \propto \nu^{\alpha_r}$), and ν_1 and ν_2 specify the frequency interval in which α_r was calculated.

fall into that part of the radio-loud regime sometimes referred to as “radio-intermediate” ($\log R \simeq 1-2$, as opposed to truly radio-loud, above $\log R \simeq 2-3$; e.g., Falcke et al. 1996), a regime in which objects are relatively rare, which classically defined the radio-loud/radio-quiet bimodality of AGNs.

2.4.2. Variability

Several sources were observed during both the NVSS and FIRST survey, and these data can be used to assess the radio variability of the galaxies. Generally, we find that NVSS and FIRST radio fluxes agree well with each other. For three sources, fluxes differ by approximately a factor of 1.6–1.8. Among these, the variability of SDSS J094857.3+002225 (integrated flux density $S_{\text{FIRST}} = 111.5$ mJy and $S_{\text{NVSS}} = 69.5$ mJy) is likely real (Zhou et al. 2003). The other two sources are Mrk 478 ($S_{\text{FIRST}} = 3.3$ mJy and

$S_{\text{NVSS}} = 5.2$ mJy) and PHL 1811 ($S_{\text{FIRST}} = 1.2$ mJy and $S_{\text{NVSS}} = 2.1$ mJy). Higher NVSS than FIRST fluxes are actually expected in the cases of very extended sources, because part of the extended emission will be missed by FIRST (e.g., Fig. 7 of White et al. 1997). Indeed, we find indications that the radio emission of PHL 1811 is extended (major axis of 2"9 reported in the FIRST catalog, and a value of <74" in the NVSS catalog). Inspecting the NVSS and FIRST images we find that Mrk 478 has a nearby bright companion source that might have slightly contributed to the NVSS radio flux estimate. Barvainis et al. (1996) report a dedicated radio observation of Mrk 478 at 1.49 GHz with $S = 4.46 \pm 0.47$ mJy, within the errors almost consistent with the NVSS and FIRST measurements.

Among those sources detected in the radio band there are 10 in the FIRST database that do not have an NVSS counterpart, while 7 in the NVSS database do not have a FIRST counterpart. The latter is just due to the nonavailability of FIRST observations at the respective coordinates. The radio images of sources with FIRST-only detections were carefully inspected by eye, and it turns out that all FIRST detections are consistent to within better than a factor of 2 with the NVSS upper limits.

2.4.3. Radio Spectral Indices

Several sources were observed in the radio regime at more than one frequency. These data can be used to estimate radio spectral shapes. Radio spectral indices α_r are reported in Table 1; α_r shows a large scatter. Steep- and flat-spectrum sources are observed. While the two galaxies SDSS J094857.3+002225 and RX J16290+4007 show very flat spectra ($\alpha_r = 0.6$ and 0.4, respectively), the majority of NLS1 galaxies are of steep-spectrum type ($\alpha_r < -0.5$).

2.4.4. Notes on Individual Objects

We comment here on the 11 apparently radio-loudest objects of this study, i.e., those falling above or close to the critical radio index, $R_{1.4} = 19$ (Fig. 1). Emphasis is put on the questions of how safely these galaxies can be called “radio-loud” (§ 2.3) and how reliable their optical spectral classification is.

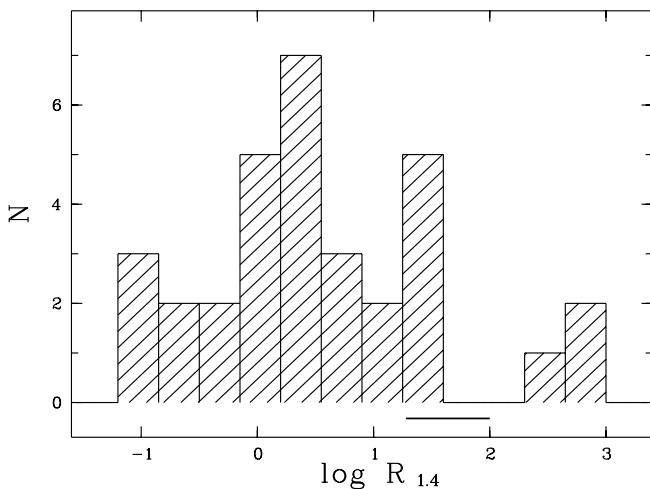


FIG. 2.—Distribution of the radio index $R_{1.4}$ of the NLS1 galaxies of our sample. The value for $R_{1.4}$ was calculated using NVSS radio fluxes and USNO-B1 m_{B2} magnitudes, except if only FIRST fluxes and/or m_{B1} magnitudes were available, which were then used. The thick horizontal bar marks the range within the radio-loud regime that is sometimes referred to as “radio-intermediate.”

TEX 1111+329: An ultraluminous infrared galaxy. Optical spectroscopy was provided by Zheng et al. (2002), who classify TEX 1111+329 as a NLS1 galaxy ($\text{FWHM}_{\text{H}\beta} \simeq 1980 \text{ km s}^{-1}$, $[\text{O III}]/\text{H}\beta = 0.75$, and $\text{Fe II}/\text{H}\beta = 1.1$). Lipari et al. (2003) report the detection of a high-velocity outflow component in $[\text{O III}] \lambda 5007$, with $v \simeq 1300 \text{ km s}^{-1}$. The galaxy is heavily absorbed, with at least $E_{B-V} = 1.08$, estimated from the observed Balmer-line ratio (Zheng et al. 2002). Assuming that this obscuration is not *intrinsic* to the line-emitting clouds (the broad-line regions [BLRs] in NLS1 galaxies might be sufficiently distant from the nucleus that dust can survive) and correcting the observed optical continuum spectrum by $A_B = 4.5$ leads to a much lower value of $R_{1.4} \simeq 20$. On the other hand, TEX 1111+329 would also be classified as radio-loud based on just its radio power, which is $P_{1.4} \simeq 10^{25} \text{ W Hz}^{-1}$. The radio spectrum declines toward higher frequencies, and TEX 1111+329 is not detected in an imaging survey at 15 GHz (Nagar et al. 2003). We keep the source as a candidate radio-loud NLS1 galaxy.

SDSS J094857.3+002225: A very radio-loud NLS1 galaxy (Zhou et al. 2003), variable in the radio and likely the optical band. Inspecting the NVSS and FIRST radio image, we noticed a second radio source very close to SDSS J094857.3+002225, FIRST J094901.5+002258, at a separation of $71''$ (corresponding to a projected distance of 395 kpc) and extended by $\sim 5''$. Suspecting it to be either a knot in a radio jet of SDSS J094857.3+002225 or a background source, we had a closer look at optical images and could not identify any optical counterpart. Closest is a faint SDSS galaxy, SDSS J094901.9+002306.4, at an offset of $10''$, an unlikely counterpart of the FIRST radio source. It is possible that the radio source has a faint, so far undetected, optical counterpart.

SDSS J172206.03+565451.6: A very radio-loud NLS1 galaxy. Depending on the choice of blue magnitude, it may be comparably radio-loud to SDSS J094857.3+002225. Its radio loudness and optical spectral properties are discussed in detail by Komossa et al. (2006). In particular, its black hole mass is unusually small given its radio loudness (Komossa et al. 2006). SDSS J172206.03+565451.6 is optically the most variable among our sample.

RX J0134–4258: A radio-loud NLS1 galaxy (Grupe et al. 2000) with peculiar X-ray spectral variability (Komossa & Meerschweinchen 2000; Grupe et al. 2000). It was detected in the PMN survey, and its radio loudness was confirmed by a dedicated follow-up observation by Grupe et al.

IRAS 20181–2244: Identified as a quasar with narrow emission lines by Elizalde & Steiner (1994). Halpern & Moran (1998) rejected a type 2 quasar classification and called it a NLS1-type object, with $\text{FWHM}_{\text{H}\beta} = 460 \text{ km s}^{-1}$ and the presence of broad wings in the Balmer lines. Kay et al. (1999) found low-level continuum polarization (2%) but no broad Balmer lines. The X-ray emission of IRAS 20181–2244 (e.g., Vaughan et al. 1999) is rapidly variable (Halpern & Moran 1998; Leighly 1999). The Balmer decrement of the narrow lines implies significant reddening (Table 1 of Halpern & Moran 1998), but the rapid X-ray variability argues against a full obscuration of the continuum source itself. The *ASCA* X-ray spectral fits indicate some excess absorption along the line of sight, and Halpern & Moran give $E_{B-V} \approx 0.3$ mag as a reasonable estimate of extinction intrinsic to IRAS 20181–2244. In the radio band, IRAS 20181–2244 is also detected in the Westerbork in the Southern Hemisphere survey at 352 MHz (de Breuck et al. 2002).

RX J16290+4007: A bright source in the X-ray (e.g., Giommi et al. 1991; Elvis et al. 1992; Brinkmann & Siebert 1994) and radio band (e.g., Giommi et al. 1991; Laurent-Muehleisen et al.

1997; White et al. 2000), likely optically variable by ~ 0.5 mag (Helfand et al. 2001). RX J16290+4007 is known as a flat-spectrum radio quasar (FSRQ). Its FSRQ nature, with respect to its X-ray and radio properties, is discussed in detail by Padovani et al. (2002). Steady TeV gamma-ray emission from RX J16290+4007 was searched for, but not detected, with the Whipple telescope (Falcone et al. 2004). Optical spectra provided by Bade et al. (1995) hinted at the NLS1 nature of RX J16290+4007, which was confirmed by Schwoppe et al. (2000) and Grupe et al. (2004).

While Padovani et al. (2002) concentrated on the radio and X-ray properties of RX J16290+4007, interpreting its relatively steep X-ray spectrum as due to synchrotron radiation and suggesting it to be the first member of a newly established class of high-energy peaked BL Lac-like FSRQs, we rather follow the alternative idea that the optical and X-ray properties of this source are driven by its *NLS1 character*.

IRAS 09426+1929: An ultraluminous object in the infrared with a single nucleus. Zheng et al. (1999) identify as a counterpart of the IR source a NLS1 galaxy at $z = 0.284$, based on an optical spectrum that shows weak $[\text{O III}]$, strong Fe II, and narrow Balmer lines (no line parameters were measured). On the one hand, the host galaxy is detected as well, and may contribute to the blue magnitude, which would make the computed value of the radio index R a lower limit. On the other hand, extinction measurements are not yet available for IRAS 09426+1929. Since the cores of ultraluminous infrared galaxies are often heavily obscured, any calculation of R based on the *observed* optical spectrum would then make the value of R an upper limit. This second effect is likely to exceed the first.

PKS 0558–504: A known radio-loud source (Remillard et al. 1986; Siebert et al. 1999), with an optical NLS1 spectrum (Remillard et al. 1986). It is highly variable in the X-ray band (e.g., Remillard et al. 1991; Gliozzi et al. 2001; Wang et al. 2001). The rapid X-ray variability and the lack of excess X-ray absorption (O’Brien et al. 2001; Brinkmann et al. 2004) indicate an unobscured view on the central engine.

RX J23149+2243: Identified as a quasar with strong Fe II emission by Wei et al. (1998). Xu et al. (2003) report emission-line measurements that indicate a relatively large width of the Balmer lines. Our newly taken spectrum (§ 3) puts the galaxy at the border between NLS1 and Seyfert 1, depending on the way the width of $\text{H}\beta$ is measured. The $[\text{O III}] \lambda 5007$ line of this galaxy shows an exceptionally strong blue wing that is blueshifted from the narrow core by 1260 km s^{-1} (§ 3). RX J23149+2243 is detected by *IRAS* and turns out to be a luminous infrared galaxy.

2E 1346+2637: An ultrasoft AGN (photon index $\Gamma_X \simeq -3.7$) at high redshift, $z = 0.92$ (Puchnarewicz et al. 1994), optically classified as a NLS1 galaxy ($\text{FWHM}_{\text{H}\beta} \simeq 1900 \text{ km s}^{-1}$, weak $[\text{O III}]$, and the presence of Fe II; Puchnarewicz et al. 1992). The X-ray spectrum of the galaxy displays one of the strongest soft excesses known. Puchnarewicz et al. (1994) report a radio upper limit of 6 mJy at 4.85 GHz and mention that this leaves a small possibility that 2E 1346+2637 is radio-loud. 2E 1346+2637 is detected by FIRST but not NVSS. The NVSS upper limit is consistent with the FIRST measurement.

SBS 1517+520: Listed as NLS1 in the VQC03, but little else is known about this galaxy (Bicay et al. [2000] reported its optical position). Our analysis of the SDSS spectrum (§ 3) does not confirm its classification as a NLS1 galaxy in the sense that $\text{FWHM}_{\text{H}\beta_g} = 3220 \text{ km s}^{-1}$ (based on a single-component Gaussian fit [Table 2]; only the “direct” determination of the width of $\text{H}\beta$, $\text{FWHM}_{\text{H}\beta_d} = 2030 \text{ km s}^{-1}$, puts it close to the

TABLE 2
SUMMARY OF OPTICAL AND X-RAY PROPERTIES OF THE RADIO-LOUD NLS1 GALAXIES OF OUR SAMPLE

NAME	$w_{H\beta}$			$w_{[O\ III]}$	[O III]	Fe II	H α	CR	Γ_X	REFERENCES
	Gaussian	Direct	Two-Component							
SDSS J094857+002225.....	1420	960	1710+ $w_{[O\ II]}$ ^a	400 ^b	0.2	1.3	...	0.04	-2.2	1
SDSS J172206+565451.....	1580	1490	1990+ $w_{[O\ III]}$	490	0.6	0.7	...	0.08	-2 to -3	1, 2
RX J0134-4258.....	930	1040	1860+ $w_{[O\ III]}$	510	0.04	3.2	3.4	0.20	-2.2 ^c	1
RX J16290+4007.....	1260	1290	1800+ $w_{[O\ III]}$	310	0.4	1.1	3.3	0.83	-3.0	1
RX J23149+2243.....	1670	1630	2680+ $w_{[O\ III]}$	620 ^d	0.2	1.4	...	0.11	-1.9	1
SBS 1517+520.....	3220	2030	3810+ $w_{[O\ III]}$	1140	1.1	0.5	...	0.015	-1.1	1
TEX 11111+329.....	1980	1480	0.75	1.1	...	<0.04	...	3
IRAS 09426+1929.....	<2000	<0.03
PKS 0558-504.....	1500	0.1	1.56 ^e	...	4.20	-2.8	4
2E 1346+2637.....	1840	1130 ^b	...	1.0	...	0.08	-3.4	5
IRAS 20181-2244.....	460	695	3.4	0.7	6.7	0.04	-2.6	6

NOTES.—The quantities $w_{H\beta}$ and $w_{[O\ III]}$ correspond to the FWHM for $H\beta$ and [O III] $\lambda 5007$, respectively, in km s^{-1} . The three entries for $\text{FWHM}_{H\beta}$ are based on a single-component Gaussian fit, a direct fit, and a two-component fit with a narrow component fixed to the same width as [O III] $\lambda 5007$, respectively. [O III] $\lambda 5007$, Fe II $\lambda 4570$, and H α are intensity ratios relative to $H\beta_g$. CR and Γ_X refer to the *ROSAT* PSPC count rate in counts per second and the soft X-ray photon index, respectively. The reference column is for the optical spectroscopy. Entries of the first six objects are based on our (re)analysis of SDSS and other spectra. The other entries were taken from the literature. In the latter case, multicomponent fits to the Balmer lines are generally not available, and only results from single-Gaussian fits to the emission lines are listed.

^a Width of narrow component fixed to that of [O II] $\lambda 3227$, since [O III] $\lambda 5007$ is too weak.

^b The reported FWHM is that of [O II] rather than [O III] (in the case of 2E 1346+2637 the [O II] width is not deconvolved from the instrumental profile).

^c During the RASS, the spectrum was significantly steeper ($\Gamma_X = -4.3$).

^d The [O III] profile has a very strong and broad blue wing. The FWHM reported here is that of the narrow core of the line only.

^e Sum of both Fe II complexes.

REFERENCES.—(1) This paper; (2) Komossa et al. 2006; (3) Zheng et al. 2002; (4) Remillard et al. 1986; (5) Puchnarewicz et al. 1994; (6) Halpern & Moran 1998.

border). Because other emission-line parameters share a similarity with those of NLS1 galaxies, we continue to include SBS 1517+520 in our tables.

3. OPTICAL SPECTROSCOPY OF THE RADIO-LOUD NLS1 GALAXIES

In order to measure the optical emission-line and continuum properties of the radio-loud NLS1 galaxies in a homogeneous way, we (re)analyzed their optical spectra when available. The spectrum of RX J0134-4258 was taken by one of us (D. G.) at ESO's 1.5 m telescope (Grupe 2004), as was the spectrum of RX J23149+2243 (D. X.), at the Xinglong 2.16 m telescope (Xu et al. 2003), while those of SDSS J094857.3+002225, SDSS J172206.03+565451.6, RX J16290+4007, and SBS 1517+520 were extracted from the SDSS database.⁷ In addition, a new spectrum of RX J23149+2243 was secured on 2005 November 25 at the 2.16 m Xinglong telescope, motivated by the remarkable structure of the [O III] $\lambda 5007$ profile of this galaxy. SDSS spectra of the other galaxies are not (yet) available. For them, emission-line data were collected from the literature when published (Table 2).

The SDSS Data Release 4 (DR4) products were used. These spectra are flux- and wavelength-calibrated by the spectroscopic pipeline in the course of the DR4 processing. The spectrum, newly taken with the 600 line mm^{-1} grating at the 2.16 m Xinglong telescope, was reduced following standard procedures (see Xu et al. 2003). The IRAF package SPECFIT (Kriss 1994) was used for spectral analysis.

We first corrected the spectra for Galactic extinction, using the Galactic E_{B-V} in the direction of the individual galaxies (Schlegel et al. 1998) and an $R = 3.1$ extinction law. We then fitted a power law to the underlying continuum using the continuum windows at 3010-3040, 3240-3270, 3790-3810, 4200-4230, 5080-5100, 5600-5630, 5970-6000, and 6005-6035 Å (Forster et al. 2001; Vanden Berk et al. 2001), known to be

relatively free from strong emission lines. The continua are generally well fitted by single power laws with indices between $\alpha = -1.3$ and -2.3 ($f_\lambda \propto \lambda^{+\alpha}$).

Since the optical-UV spectra of all sources show emission from Fe II complexes, an Fe II spectrum was then fitted and subtracted (excluding the UV Fe II multiplets around Mg II $\lambda 2798$, which are not included in the template) using the optical Fe II template and the technique described by Boroson & Green (1992).

The Fe II- and continuum-subtracted spectra were then used to measure emission-line properties. The emission lines were modeled by single-Gaussian profiles or combinations of Gaussian and Lorentzian profiles. The approach was to fit single-component Gaussian profiles to the weak forbidden lines, apply two-component Gaussian profiles to [O III] when necessary, and compare double-Gaussian and Gaussian-plus-Lorentzian profiles in their success in representing the H α and $H\beta$ line profiles. In addition, a direct measurement of the $H\beta$ line width was performed (without any assumption about line profile shape). $H\beta$ line results are marked with an index “g” or “d” if referring to a Gaussian fit or the direct method, respectively, and with a “b,” “n,” or “tot” when referring to the broad, narrow, or whole emission component, respectively, of a two-Gaussian decomposition of the line profile.

Results for the diagnostically most important emission lines are listed in Table 2. For the sake of simplicity and homogeneity, the listed emission-line ratios are based on single-Gaussian fits to the lines, even though for some sources this is not a perfect match of the line profile. The instrumental resolution was corrected for in the FWHMs measured by us. We confirm the NLS1 classification for almost all galaxies, with the possible exceptions of SBS 1517+520 and RX J23149+2243 (see below). Line widths of confirmed NLS1 galaxies range over $\text{FWHM}_{H\beta_g} = 930-1580 \text{ km s}^{-1}$, while the flux ratio [O III]/ $H\beta_g$ varies between 0.04 and 1.1 (results from Gaussian fits are reported here). Fe II is detected in all spectra and ranges over $\text{Fe II } \lambda 4570/H\beta_g = 0.5-3.2$ ($\text{Fe II } \lambda 4570/H\beta_{\text{tot}} = 0.5-2.4$). The NLS1 galaxies of our sample cover almost the whole range of Fe II $\lambda 4570/H\beta$ observed in

⁷ See <http://cas.sdss.org/dr4/en/tools/explore/obj.asp>.

the NLS1 population (e.g., Table 3 of Véron-Cetty et al. 2001), except that the lowest $\text{Fe II}/\text{H}\beta$ ratios are missing in our sample.

SBS 1517+520 and RX J23149+2243 have rather broad Balmer lines, and it depends on the way the profile of $\text{H}\beta$ is fitted whether or not they formally fulfill the criterion of $\text{FWHM}_{\text{H}\beta} < 2000 \text{ km s}^{-1}$. Both of them have $\text{FWHM}_{\text{H}\beta_b} > 2000 \text{ km s}^{-1}$, while $\text{FWHM}_{\text{H}\beta_d} < 2000 \text{ km s}^{-1}$. While the strict cut in FWHM is a useful working criterion for extraction of NLS1 galaxy candidates from larger samples, it has been repeatedly noted that the cut value is not well defined or even completely arbitrary. Véron-Cetty et al. (2001) suggested that a better classification criterion than $\text{FWHM}_{\text{H}\beta}$ may actually be the Fe II ratio, $\text{Fe II } \lambda 4570/\text{H}\beta_{\text{tot}} > 0.5$. According to this criterion, both SBS 1517+520 and RX J23149+2243 are still classified as NLS1 galaxies. After these cautious comments, we continue to keep the two galaxies in the sample, even though they fail a strict $\text{FWHM}_{\text{H}\beta_b} > 2000 \text{ km s}^{-1}$ criterion.

RX J23149+2243 is exceptional in showing a very strong and broad blue wing in the $[\text{O III}] \lambda 5007$ and $[\text{O III}] \lambda 4959$ lines. The presence of the blue wing was hinted at in the earlier low-resolution spectrum of Xu et al. (2003) and was confirmed in the new spectrum we took in 2005 November (full results on this galaxy will be presented elsewhere). $[\text{O III}] \lambda 5007$ is well modeled by two Gaussian lines. The core, with $\text{FWHM}_{[\text{O III}]_n} = 620 \text{ km s}^{-1}$, is at the same redshift as the peak of $\text{H}\beta$, while the wing, with $\text{FWHM}_{[\text{O III}]_b} = 1560 \text{ km s}^{-1}$, is highly blueshifted by 1260 km s^{-1} . SBS 1517+520 also shows a blue wing in $[\text{O III}]$. The line is well fitted by two Gaussian profiles with $\text{FWHM}_{[\text{O III}]_n} = 610 \text{ km s}^{-1}$ and $\text{FWHM}_{[\text{O III}]_b} = 2070 \text{ km s}^{-1}$, blueshifted by $v = 90 \text{ km s}^{-1}$. In the SDSS spectra of the other objects of our sample, the blue wing is present but not exceptionally strong. For SDSS J172206.03+565451.6 the line blueshift is $v = 140 \text{ km s}^{-1}$, and for RX J16290+4007 we measure $v = 230 \text{ km s}^{-1}$.

4. X-RAY SPECTROSCOPY AND VARIABILITY

While some of the sources of our sample have no previous X-ray studies, others (in particular, PKS 0558–504) have been observed by most major X-ray satellites. In order to obtain representative X-ray fluxes of all our sources in a homogeneous way, including upper limits for nondetected sources, we make use of the data obtained with the PSPC (Positional Sensitive Proportional Counter) in the *ROSAT* All-Sky Survey (RASS; Voges et al. 1999) and the later phase of pointed observations.

Nine out of the 11 sources have X-ray detections, eight of these in the RASS and three in pointed observations. Count rates and hardness ratios were obtained for all sources. Fixing the absorption at the Galactic values in the directions of the individual sources, hardness ratios were then converted to power-law indices, and the absorption-corrected fluxes in the (0.1–2.4) keV band were determined. Power-law indices were in the range $\Gamma_X = -1.9$ to -4.3 (Table 2), with the exception of the faint source SBS 1517+520 ($\Gamma_X = -1.1$; likely caused by excess absorption). In cases in which pointed observations existed (RX J16290+4007, 2E 1346+2637, and RX J0134–4258), these were given preference over the RASS data.

For the two nondetected sources, TEX 1111+329 and IRAS 09426+1929, upper limits were obtained. However, we caution that while soft X-ray nondetections convert into safe upper limits for nonobscured sources, the same is not true for obscured sources. This is likely the case for both TEX 1111+329 and IRAS 09426+1929. For completeness, we report the 2σ upper limits on the soft (0.1–2.4 keV) X-ray count rates in Table 2, but we do not convert them into luminosities and do not use them for accretion rate estimates.

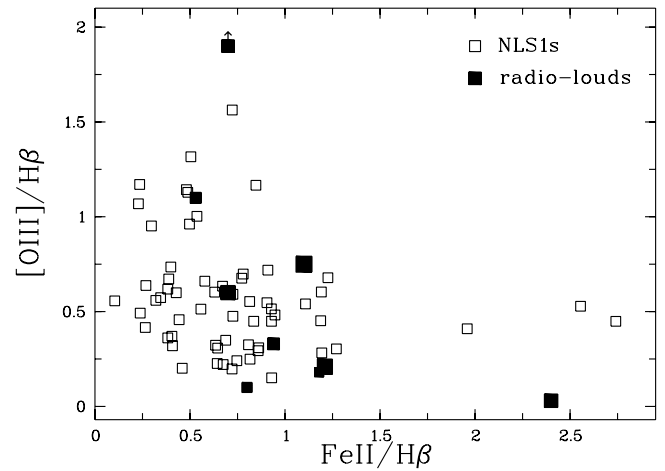


FIG. 3.—Distribution of the radio-loud NLS1 galaxies of our sample (filled squares) in the $(\text{Fe II}/\text{H}\beta_{\text{tot}}, [\text{O III}]/\text{H}\beta_{\text{tot}})$ diagram of NLS1 galaxies (open squares; Xu et al. 2006). Square size scales with radio loudness; the larger the square diameter the radio-louder the source. The source IRAS 20181–2243 is off the plot, indicated by the arrow.

We also inspected the RASS X-ray light curves of the X-ray-brighter sources and found that most are consistent with a constant source flux except for PKS 0558–504, which shows repeated flaring activity. Variability of the X-ray-fainter sources cannot be judged due to the poor statistics.

5. DISCUSSION

Judged on radio index, 11 objects can be classified as radio-loud NLS1 galaxies or candidates. Our study almost triples the number of recognized radio-loud NLS1 galaxies if the candidates close to the dividing line are confirmed. Implications of the new results are discussed below.

5.1. Comparison of the Properties of the Known Radio-loud NLS1 Galaxies

Even though the number of known radio-loud NLS1 galaxies and candidates is still small, we have enough objects now to compare their X-ray, optical, and radio properties to have a first assessment of their similarities or differences. In particular, we checked whether the ~ 11 radio-loud NLS1 galaxies are extreme in one or more of their multiwavelength spectral properties, i.e., whether they differ significantly from the radio-quiet galaxies in their properties, and whether there is a trend *within* the sample such that one or more properties correlate with radio loudness.

Among optical emission lines, the “first eigenvector” (Boroson & Green 1992) is evident among the objects of our sample in that weak $[\text{O III}]/\text{H}\beta$ emission tends to go hand-in-hand with strong Fe II emission and vice versa. Both $[\text{O III}]/\text{H}\beta$ and $\text{Fe II}/\text{H}\beta$ vary strongly across the sample, almost spanning the whole range observed in NLS1 galaxies. In Figure 3 we plot the location of the radio-loud NLS1 galaxies in the $(\text{Fe II}, [\text{O III}])$ diagram, in comparison with one of the largest homogeneously analyzed optical NLS1 samples available to date (Xu et al. 2006). We do not find a strong correlation of any of the parameters with radio loudness, but larger samples are needed to confirm this.

Even though radio loudness did not occur in the sample of Marziani et al. (2001) for line widths $\text{FWHM}_{\text{H}\beta_b} < 4000 \text{ km s}^{-1}$, the radio-loud galaxies of our sample do populate regions similar to those of other AGNs in the $(\text{FWHM}_{\text{H}\beta_b}, \text{Fe II})$ diagram (Fig. 4 of Marziani et al. 2001) and extend the range in which radio

loudness is observed to significantly smaller FWHMs than previously known (see also § 5.5).

Given suggestions that the blue wings in the [O III] λ 5007 line of quasars are sometimes linked to interactions of the radio plasma with the narrow-line region clouds (Leipski & Bennert 2006 and references therein), we paid special attention to the existence and strengths of blue wings in dependence on radio loudness but did not find any correlation, even though 2–3 out of the 11 sources do show very intense blue wings, two with strong blueshifts, among the highest values ever observed.

Most NLS1 galaxies of our sample have steep radio spectra (Table 1) in the frequency band 0.33–1.4–4.85 GHz,⁸ and their radio emission is compact. As such, they share some similarity with compact steep-spectrum (CSS) sources (Peacock & Wall 1982), which are believed to be young radio sources that have not yet evolved strongly (Marecki et al. 2006 and references therein). SDSS J094857.3+002225 and RX J16290+4007 have inverted radio spectra. Only one source, SDSS J094857.3+002225 (Zhou et al. 2003), shows significant variability in the radio band by a factor of ~ 1.6 .

Soft X-ray spectra are generally steep but come with large errors. The mean *ROSAT* power-law index of the radio-loud NLS1 galaxies of our sample⁹ (excluding SBS 1517+520, which has an unusually flat index), $\Gamma_X = -2.7$, is similar to that of soft X-ray-selected NLS1 galaxies ($\Gamma_X = -2.96 \pm 0.41$; Grupe et al. 2004). PKS 0558–504 (e.g., Remillard et al. 1991), IRAS 20181–2244 (Halpern & Moran 1998), and RX J16290+4007 (Padovani et al. 2002) are highly variable in the X-ray band, while RX J0134–4258 strongly changed its spectral shape (Grupe et al. 2000; Komossa & Meerschweinchen 2000).

5.2. Starburst Contribution?

It has been suggested that NLS1 galaxies are AGNs in an early phase of evolution. This includes the possibility of enhanced starburst activity in these objects (e.g., Mathur 2000; Shemmer et al. 2004). Could starbursts contribute to or dominate the radio power of the radio-loud NLS1 galaxies of our sample? Generally, normal and starburst galaxies are much less luminous than quasars in the radio regime. In particular, all of our NLS1 galaxies also exceed the radio powers of a sample of the most radio-luminous starbursts, all of them in luminous and ultraluminous infrared galaxies (Smith et al. 1998): $\log P_{4.85, \text{SB}} \simeq 22.3\text{--}23.4 \text{ W Hz}^{-1}$. Radio powers place all of our NLS1 galaxies with $R_{1.4} > 19$ in the radio-loud regime ($\log P > 24$; Joly 1991), some of them close to the lower border, however.

At first glance a significant starburst contribution might be suspected for the two ultraluminous infrared galaxies among our sample, TEX 11111+329 and IRAS 09426+1929. We used the tight correlation between IR luminosity and radio luminosity of starburst galaxies (Yun et al. 2001 and references therein) to predict the expected starburst radio power, given the 60 μm IR luminosities of these two galaxies measured by *IRAS*. According to equation (4) of Yun et al. (2001), with $\log P_{1.4, \text{NVSS}} \simeq 25 \text{ W Hz}^{-1}$ TEX 11111+329 exceeds by a factor of 10 the contribution expected from a starburst, while for IRAS 09426+1929 the measured radio power, $\log P_{1.4, \text{NVSS}} \simeq 24.7 \text{ W Hz}^{-1}$, is a factor of 5 above the predicted starburst contribution. TEX 11111+329 has radio observations at several frequencies. The spectral index

is relatively steep but comparable to other sources of our sample. The spectral index between 0.33 and 1.4 GHz is similar to SDSS J172206.03+565451.6 and PKS 0558–504, while toward higher frequencies it is comparable to RX J0134–4258.

The same comparison between observed radio power and expected starburst contribution was done for the three other galaxies with *IRAS* 60 μm flux measurements. We found that the observed radio powers of PKS 0558–504, IRAS 20181–2244, and RX J23149+2243 exceed by factors of 115, 6, and 6, respectively, the predicted starburst contribution.

We conclude that radio-luminous starbursts are unlikely to dominate the radio emission of most of our sources.

5.3. Black Hole Masses

Reverberation mapping of Seyfert galaxies established a relation between the radius of the BLR and the optical luminosity (Kaspi et al. 2005; Peterson et al. 2004; and references therein). Assuming that the BLR clouds are virialized (e.g., Wandel et al. 1999), the black hole mass can then be estimated as $M_{\text{BH}} = G^{-1} R_{\text{BLR}} v^2$. The BLR radius, R_{BLR} , in dependence on the optical luminosity at 5100 \AA , is given by $R_{\text{BLR}} = 22.3 [\lambda L_{\lambda}(5100 \text{ \AA}) / 10^{44} \text{ ergs s}^{-1}]^{0.69} \text{ lt-days}$ (eq. [2] of Kaspi et al. 2005). The velocity v of the BLR clouds is usually estimated from the FWHM as $v = f \times \text{FWHM}$, where $f = \sqrt{3}/2$ for an isotropic cloud distribution. While the relation is now well established for nearby Seyfert galaxies, few NLS1 galaxies have been reverberation mapped so far (Peterson et al. 2000). Following standard practice, we assume equation (2) of Kaspi et al. (2005) is indeed applicable to NLS1 galaxies as well, and proceed in estimating the black hole masses of our sample.

The luminosity $L_{\lambda}(5100 \text{ \AA})$ was derived from the SDSS spectra (corrected for Galactic extinction) when available, or else estimated from blue magnitudes m_{B2} of the USNO-B1 catalog. (Note that some of the galaxies of our sample vary in the optical band, which introduces an uncertainty in the black hole mass estimates. Most objects, however, vary by less than a factor of 2.) The FWHM of the broad component from the two-component fit of H β was used for the black hole mass estimates reported in Table 3 when optical spectra were available. Otherwise, results for the FWHMs from single-component line fits collected from the literature (Table 2) were used for an order-of-magnitude estimate.

We obtained black hole masses in the range $M_{\text{BH}} \simeq (2\text{--}10) \times 10^7 M_{\odot}$ (objects with two-component decomposition of H β available) and $M_{\text{BH}} \simeq (0.2\text{--}9) \times 10^7 M_{\odot}$ (objects with single-component fits to H β ; this underestimates FWHM $_{\text{H}\beta}$, and therefore underestimates the black hole mass) for our sample. These masses are surprisingly small, given the radio loudness of the galaxies (Fig. 4). In fact, all galaxies fall right into an unpopulated regime of the Laor diagram (Fig. 2 of Laor 2000), which plots radio loudness versus black hole mass. While larger samples filled up some originally empty areas in the Laor diagram, and while some discussion has emerged about whether there is any clear dependence of black hole mass on radio loudness at all (e.g., Lacy et al. 2001; Oshlack et al. 2002; Woo & Urry 2002; McLure & Jarvis 2004; Best et al. 2005), our radio-loud NLS1 galaxies are still located in an area very sparsely populated by galaxies, first because the black hole masses are unusually small given the radio loudness of the galaxies of our sample (e.g., Fig. 2 of Laor 2000; Fig. 3 of Lacy et al. 2001; Fig. 2 of McLure & Jarvis 2004; Fig. 10 of Metcalf & Magliocchetti 2006), and second because most radio indices R of our objects are in a range that is classically known to be less populated by quasars, which defined the radio-loud/radio-quiet bimodality of AGNs (with radio-quiet

⁸ The nonsimultaneity of the data, taken with different instrumental configurations, has to be kept in mind, but it is unlikely that all scatter in α_r among the sample can be traced back to variability, or else variability in individual cases would be huge.

⁹ Note that a number of them were first identified by X-ray observations.

TABLE 3
ESTIMATED BLACK HOLE MASSES AND EDDINGTON RATIOS

Name	M_{BH} (M_{\odot})	$10L_{\text{X}}/L_{\text{Edd}}$	Comments
SDSS J094857+002225.....	4×10^7	4.5	Source might be beamed; see also Zhou et al. (2003)
SDSS J172206+565451.....	3×10^7	3	
RX J0134–4258.....	4×10^7	1	
RX J16290+4007.....	2×10^7	7	Source might be beamed
SBS 1517+520.....	1×10^8	0.07	Likely X-ray-absorbed; $L_{\text{X}}/L_{\text{Edd}}$ is lower limit
RX J2314+2243.....	8×10^7	0.2	
PKS 0558–504.....	9×10^7	7	See also Wang et al. (2001)
TEX 11111+329.....	2×10^7	...	Likely optically absorbed
IRAS 09426+1929.....	$<9 \times 10^7$...	$\text{FWHM}_{\text{H}\beta} < 2000 \text{ km s}^{-1}$ assumed; probably optically absorbed
2E 1346+2637.....	8×10^7	4	
IRAS 20181–2244.....	3×10^6	6	

NOTES.—Data are for NLS1 galaxies with SDSS or other spectra (first six objects; the broad component of $\text{H}\beta$ is used for the black hole mass estimate) and for other NLS1 galaxies (single-Gaussian fits to $\text{H}\beta$ from the literature are used for black hole mass estimates).

quasars below $R \approx 1–10$ and many radio-loud quasars above $R \approx 100–1000$; e.g., Fig. 10 of Woo & Urry 2002). An even more extreme outlier is PKS 2004–447, which shows a lower black hole mass and higher radio index R than objects of our sample (Oshlack et al. 2001).

While of unusually low mass when compared to radio-loud quasars, *among the NLS1 population itself* our radio-loud NLS1 galaxies are actually at the *high-mass end* (for comparison, in the sample of Grupe & Mathur [2004] NLS1 masses range between 6×10^5 and $4 \times 10^7 M_{\odot}$, with only one object around $10^8 M_{\odot}$). To some extent, the lack of higher mass black holes among NLS1 galaxies in general may just be a selection effect that arises from the standard definition of NLS1 galaxies as objects with $\text{FWHM}_{\text{H}\beta} < 2000 \text{ km s}^{-1}$. Since there is a clear correlation between $\text{H}\beta$ luminosity and $\text{H}\beta$ width (e.g., Fig. 15 of Véron-Cetty et al. 2001), higher luminosity AGNs would have broader Balmer lines, finally exceeding $\text{FWHM} > 2000 \text{ km s}^{-1}$, and thus would no longer be called NLS1 galaxies. Ideally, any

NLS1-defining criteria should incorporate that effect (Wills et al. 2000).

In any case, while we cannot exclude that NLS1 galaxies with higher black hole masses do exist, the fact that the radio-loud objects of our sample cluster in a previously almost unpopulated parameter space of M_{BH} and R is still remarkable. We caution that there are indications that two to three galaxies of the sample are actually beamed sources (§ 5.7.1). Any contribution of beamed emission to the optical band makes our estimate of black hole mass an *upper limit*, while, on the other hand, we *underestimate* the black hole mass if the BLR clouds are arranged in a disk rather than a sphere (Vestergaard et al. 2000). Among the sources of our sample, SDSS J172206.03+565451.6 is the radio-loudest with “reliable” radio index measurement, since there are no indications for beaming and likely no absorption in the optical band (Komossa et al. 2006).

5.4. Accretion Rate

With knowledge of black hole mass and X-ray luminosity it is possible to perform an estimate of the accretion luminosity relative to the Eddington value. We intentionally use the X-ray luminosity here, and we do not apply any bolometric correction, since it is unlikely to be constant for all NLS1 galaxies, and since, in particular, the extreme-UV (EUV) part of their spectral energy distribution (SED) is unknown.¹⁰

We find that the ratio of 0.1–2.4 keV luminosity to Eddington luminosity (Table 2) ranges between $L_{\text{X}}/L_{\text{Edd}} = 0.02$ (RX J23149+2243) and 0.7 (RX J16290+4007) *without* any bolometric correction, which might typically be an additional factor of 5–10 (Tables 14 and 15 of Elvis et al. 1994). An exception is SBS 1517+520, with $L_{\text{X}}/L_{\text{Edd}} = 0.007$. We suspect that this very faint X-ray source is absorbed in X-rays by a (dust-free) absorber, which would also explain its very flat power law with index $\Gamma_{\text{X}} \approx -1.1$, which is formally obtained when fixing the absorption at the Galactic value. We excluded TEX 11111+329 and

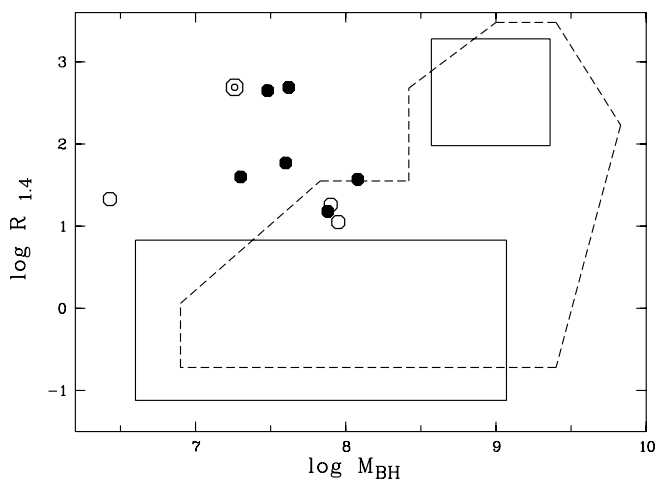


FIG. 4.—Dependence of radio loudness on black hole mass for the radio-loud NLS1 galaxies of our sample for which spectra were available to us (*filled circles*) and based on spectra in the literature (*open circles*). The solid and dashed lines mark areas populated by the bulk of the radio sources of the samples of Laor (2000) and Lacy et al. (2001), respectively. The open double circle marks TEX 11111+329, which is possibly strongly absorbed. See the text for further details, including comments on individual sources. If both FIRST and NVSS radio observations were available, radio indices shown in this plot were calculated based on the NVSS data.

¹⁰ There have been suggestions that the X-rays connect in one “big blue bump” to the optical band on the one hand, but findings that NLS1 galaxies are underluminous in the UV on the other hand, and inspections of individual objects, lead to expectations of flat EUV SEDs in some cases and soft excesses in other cases. Ideally, bolometric corrections would therefore be done for each object individually based on a measurement of the multiwavelength SED on the one hand and detailed emission-line modeling on the other hand in order to constrain the EUV part of the SED from emission-line ratios and $\text{H}\beta$ line flux.

IRAS 09426+1929 from this estimate since no meaningful X-ray upper limit could be obtained.

For comparison with $L_{\text{bol}}/L_{\text{Edd}}$ values reported in the literature, we also estimated bolometric luminosities based on the optical luminosity at 5100 Å and a constant bolometric correction factor of 9 (e.g., § 2 of Warner et al. 2004; Greene et al. 2006); i.e., $L_{\text{bol}} = 9\lambda L_i(5100 \text{ Å})$. This gives an average $L_{\text{bol}}/L_{\text{Edd}} = 1.2$ (again excluding TEX 11111+329 and IRAS 09426+1929, plus IRAS 20181–2244), which is higher than the NLS1 average of Warner et al. (2004; 0.67, but note that they used C IV $\lambda 1549$ rather than H β for black hole mass estimates) but not as high as observed in the most luminous quasars (e.g., Warner et al. 2004; Shemmer et al. 2004).

5.5. Radio–Fe II Connection, Comparison with Population A/B Sources, and the Radio-loud/Radio-quiet Bimodality in Eigenvector 1

Among *broad-line* quasars the nature of the Fe II emission has been much discussed in the literature with respect to radio properties (e.g., Joly 1991; Miller et al. 1993). Two models were considered to explain the connection between radio and Fe II emission in radio-loud sources: an orientation-dependent model of Fe II emission (e.g., Jackson & Browne 1991) and a jet model in which Fe II is produced when the jet interacts with the ambient medium (Joly 1991). Boroson & Green (1992) and Boroson (2002) find that radio loudness is statistically linked to the physical parameters that drive eigenvector 1 in the sense that quasars with strong [O III] and weak Fe II are preferentially radio-loud, while strong Fe II emitters are generally radio-quiet objects (for an example of an exception, see Zhou et al. 2002).

The radio-loud NLS1 galaxies of our sample do not fit in this scheme in the sense that their Fe II emission does not show a clear dependence on radio loudness but almost covers the whole observed range in NLS1 galaxies (Fig. 3; cf. Fig. 4 of Marziani et al. 2001). In particular, RX J0134–4258, about the fourth radio-loudest of our sample, is one of the strongest Fe II emitters known.

Sulentic et al. (2003) demonstrate that the radio-loud/radio-quiet distinction of AGNs is obvious in their eigenvector 1, which links the width of the broad component of H β with the equivalent-width ratio of Fe II to H β (their Fig. 3), in the sense that radio-loud and radio-quiet objects occupy different domain spaces. NLS1 galaxies are not among their sample. Sulentic et al. define two populations of AGNs according to their emission-line properties. Population A is sources with $\text{FWHM}_{\text{H}\beta} < 4000 \text{ km s}^{-1}$, while $\text{FWHM}_{\text{H}\beta} > 4000 \text{ km s}^{-1}$ in population B sources. In their sample, radio loudness is almost exclusively confined to population B. The radio-loud NLS1 galaxies of our sample fall into the rarely populated regime of Figure 3 of Sulentic et al., most of them in the “gap” between radio-loud and radio-quiet galaxies, but not to an extent that the bimodality is obliterated.

5.6. Inclination

Orientation plays an important role in AGN unification scenarios of both Seyfert galaxies (Antonucci 1993; Elvis 2000) and radio galaxies (Urry & Padovani 1995). Inclination also enters black hole mass and accretion rate estimates and consequently affects black hole mass–bulge mass relations of NLS1 galaxies and their cosmological implications (see, e.g., the discussion in Collin & Kawaguchi 2004).

The orientation of NLS1 galaxies with respect to our line of sight has repeatedly been addressed, and arguments and evidence in favor of and against a pole-on view have been presented. Originally, for instance, a pole-on view was suggested to explain the small width of the Balmer lines (e.g., Osterbrock &

Pogge 1985; Puchnarewicz et al. 1992; Bian & Zhao 2004). The disk emission of Fe II is also anisotropic, and Fe II emission is strongest when the disk is viewed face-on (e.g., Miller et al. 1993; Marziani et al. 2001). A pole-on orientation was also suggested for individual NLS1 galaxies with extreme variability (e.g., PKS 0558–504; Remillard et al. 1991). Correcting for these orientation effects, systematic or random in nature, is also important in the context of black hole mass estimates and black hole mass–bulge mass relations of NLS1 galaxies, which make use of Balmer line widths. On the other hand, Smith et al. (2005) argued that, based on their polarization properties, there are no indications that NLS1 galaxies are preferentially viewed face-on.

Radio observations of NLS1 galaxies allow us to re-address orientation issues. Among our sample, there are two to three NLS1 galaxies that are likely beamed (SDSS J094857.3+002225, RX J16290+4007, and possibly PKS 0558–504; § 5.7.1), implying a pole-on view into the central engine. If the width of the Balmer lines was dominated by orientation, we would then expect these objects to show very narrow Balmer lines. However, this is not the case ($\text{FWHM}_{\text{H}\beta} = 1710$ and 1800 km s^{-1} , respectively, for SDSS J094857.3+002225 and RX J16290+4007). Larger samples of beamed NLS1 galaxies are needed to put this on a firmer statistical basis.

5.7. Frequency of Radio-loud NLS1 Galaxies

Of the 128 NLS1 galaxies in the VQC03 catalog, 90% are located within the NVSS area. Among these, 7% are formally radio-loud ($R_{1.4} \gtrsim 19$), while only 2.5% exceed $R = 100$. One or a few of these sources are most likely significantly absorbed, and one or two are at the border between Seyfert 1 and NLS1 galaxies. Given a fraction of $\sim 13\%$ – 20% of radio-loud galaxies among optically selected quasars (e.g., Visnovsky et al. 1992; La Franca et al. 1994; Falcke et al. 1996), radio-loud NLS1 galaxies are more rare than radio-loud quasars.

In order to compare directly the fraction of radio-loud galaxies among narrow-line and broad-line type 1 quasars listed in the VQC03, we have also extracted the broad-line quasars from the VQC03, cross-correlated them with the NVSS catalog, and determined the fraction of radio-loud galaxies the same way we did for the NLS1 galaxies. We find that $\sim 90\%$ of the objects are located within the NVSS area. Among these, $\sim 20\%$ are radio-loud ($R_{1.4} \gtrsim 19$), and $\sim 14\%$ exceed $R = 100$. Again, this indicates a lack of radio-loud galaxies among NLS1 galaxies, particularly at high values of radio index R .

When comparing the frequency of radio-loud NLS1 galaxies with radio-loud type 1 quasars, two things have to be kept in mind. First, the mere definition of NLS1 galaxies as objects with $\text{FWHM}_{\text{H}\beta} < 2000 \text{ km s}^{-1}$ likely biases the observed black hole mass distribution toward excluding the most massive black holes. Since there are indications that radio-loud AGNs have, on average, higher black hole masses (e.g., Metcalf & Magliocchetti 2006), we may automatically miss some of the most massive radio-loud NLS1 galaxies because they escape the definition as NLS1 galaxies and are rather called Seyfert 1.

Second, specific to the present sample, great attention was paid to each single object in that cautious comments were issued in the case of evidence for excess extinction, and in that line profiles were fitted with a number of different models. The same detailed object-by-object analysis should be applied to comparison samples of quasars when citing the fraction of radio-loud quasars in comparison with that of radio-loud NLS1 galaxies.

Keeping this in mind, it still appears that radio-loud NLS1 galaxies are less abundant than radio-loud quasars, and we proceed in attempting to explain this distinction.

The cause of radio loudness in quasars is still unknown, even though a number of different models have been suggested and investigated, including the influence of spin (e.g., Wilson & Colbert 1995; Blandford 2000; Ye & Wang 2005), black hole mass (e.g., Laor 2000; Metcalf & Magliocchetti 2006), the rate of cooling gas in the host galaxy (Best et al. 2005), and beaming in radio-intermediate FSRQs, which have been suggested to be relativistically boosted radio-quiet galaxies (Miller et al. 1993; Falcke et al. 1996).

Two key questions regarding the radio properties of the NLS1 galaxies are: Why is the phenomenon of radio loudness more rare in NLS1 galaxies than in quasars? And, related to that: Is the mechanism that drives the radio loudness the same in both types of objects, or is a fundamentally different mechanism at work in the few radio-loud NLS1 galaxies? We discuss several models in turn.

5.7.1. Beaming

We first explore the possibility that NLS1 galaxies might be radio-quiet but intrinsically beamed sources. In this scenario, one then expects that other optical and X-ray properties of the radio-loud NLS1 galaxies are affected as well. For instance, Fe II emission might then be extreme. This holds for both scenarios, either when originating in a disk that is viewed face-on (e.g., Miller et al. 1993) or when there is an additional contribution to Fe II induced by the interaction of the jet with ambient matter (e.g., Joly 1991). Also, X-ray soft excess emission is expected to be stronger if the sources are viewed face-on for the case of a geometrically thick accretion disk (Madau 1988). At the same time there might be a flatter nonthermal contribution to X-rays from the jet emission.

While a few sources of our sample are indeed good candidates for beaming, others are not. RX J16290+4007 and SDSS J094857.3+002225 are likely beamed, but only RX J16290+4007 is radio-intermediate. RX J16290+4007 likely is a blazar of FSRQ type (e.g., Padovani et al. 2002), and SDSS J094857.3+002225 exhibits strong variability in the radio band (Zhou et al. 2003). These are the only two sources among our sample with very flat radio spectra (Table 1). Apart from that, PKS 0558–504 exhibits unusual X-ray flaring activity, and there have been repeated speculations that this may be related to beaming effects in a jet (Remillard et al. 1991; Gliozzi et al. 2001; Wang et al. 2001). An origin in the accretion disk is an alternative, however, and this latter model is preferred by Wang et al. (2001) and by Brinkmann et al. (2004) to explain the *XMM-Newton* data.

Other sources of our sample are steep-spectrum radio sources from which strong beaming is generally not expected. X-ray spectra are steep (even those of the two FSRQs), arguing against the dominance of a nonthermal Doppler-enhanced contribution to the soft X-ray spectrum. Beamed sources more typically show $\Gamma_X \simeq -1.5$ to -1.6 .

5.7.2. Accretion Mode

While estimated Eddington accretion rates are in line with other findings that NLS1 galaxies are accreting close to or above their Eddington limit, the radio loudness of such sources is unexpected at first glance, given observations that radio emission is suppressed in accretion high states in some types of Galactic and extragalactic sources. According to Maccarone et al. (2003 and references therein), Galactic X-ray binaries in soft/high states and AGNs show quenched radio emission for relatively high accretion rates. Even though the analogy between Galactic black holes and NLS1 galaxies has been drawn repeatedly (e.g., Pounds et al. 1995), it is still unclear how far it reaches. Greene et al. (2006 and references therein) more generally suggested that radio loud-

ness is anticorrelated with $L_{\text{bol}}/L_{\text{Edd}}$ (their Fig. 3) in a sample of Seyfert galaxies and PG quasars, albeit with quite some scatter. Whether this trend still holds for high-redshift, highly accreting quasars has yet to be explored. So far, these observations suggest that the mechanism that suppresses the radio emission for high $L_{\text{bol}}/L_{\text{Edd}}$ could also be responsible for the lower fraction of radio-loud galaxies among NLS1 galaxies.

While it is generally agreed on that jet formation (and thus radio emission) is intimately linked to the presence and structure of an accretion disk, the actual mechanism of launching a jet from the inner disk regions is not yet really understood (see, e.g., Celotti & Blandford [2001] and Meier [2003] for recent reviews). One may speculate that the observed differences originate from differences in the accretion mode between stellar mass and supermassive black hole accretors and between different classes: It is generally agreed on that at relatively low accretion rates (in terms of the Eddington rate), radiatively inefficient accretion flows prevail (e.g., Beckert & Duschl 2002). Independent of not yet fully understood details of these flows, they seem to be potentially efficient in producing radio emission themselves (e.g., Yi & Boughn 1998; Narayan et al. 1998). At rates closer to but still well below the Eddington limit, disks turn optically thick and geometrically thin (see Wang et al. [2003] for a suggestion how radio emission might be enhanced in this case). Barring details at these low accretion rates, the properties of the flows seem to be rather similar between stellar mass and supermassive black hole accretors.

When the accretion rate reaches or even surpasses the Eddington rate, however, the physical state of the accretion process becomes less clear. One has to keep in mind that the Eddington rate has been derived for a perfectly spherically symmetric situation. The situation in accretion disks, however, is rather different from such an ideal case. While at rates close to the (spherical) Eddington limit accretion disks in all likelihood are no longer geometrically thin (slim disks; see, e.g., Collin & Kawaguchi 2004), their deviation from sphericity is even more important. This can lead to simple geometric effects allowing for super-Eddington accretion rates (D. Heinzeller & W. J. Duschl 2006, in preparation) but also to instabilities in the structure of the disks, for instance, the photon bubble instability as discussed by Begelman (2002), and in all likelihood to combinations of such geometric and physical effects (e.g., Okuda et al. 2005).

An additional potentially relevant difference between stellar mass and supermassive black hole accretors may be the mass of the disk. While in the stellar case the masses of the accretion disk are certainly well below that of the accreting body, this is considerably less clear for the AGN case, and may even be different for different AGN types. In the innermost disk regions, self-gravity certainly plays no role. Already at moderately large radii, however, this may change. With such changes, long-term modifications of the mass supply rate for the inner regions comes along. Different levels of self-gravity in the disks may very well lead to differences in the accretion process.

Therefore, different accretion modes have the potential to explain the observed differences in radio loudness between Galactic and AGN sources on the one side, and among the different AGN classes on the other side. However, before one can unambiguously identify whether any, and if so which, aspect of the accretion mode gives rise to the differences, a much better understanding is required of how these different accretion modes relate to jet formation.

5.7.3. Black Hole Spin

Another parameter that could account for radio loudness but at the same time leave optical emission-line parameters and

correlations mostly unaffected is black hole spin. It is expected to have a strong direct influence on radio jet emission if the radio jet is powered by the extraction of black hole rotational energy (Blandford & Znajek 1977), or may indirectly be relevant if the jet is powered by the rotational energy of the inner disk (Blandford & Payne 1982).

If, indeed, rapidly spinning black holes are responsible for radio loudness of NLS1 galaxies and quasars, why then would NLS1 galaxies *on average* harbor *less* rapidly spinning black holes than Seyfert galaxies (to account for the lower frequency of radio loudness among NLS1 galaxies)? Both black hole–black hole mergers and accretion will affect black hole spin (e.g., Merritt 2002; Hughes & Blandford 2003; Volonteri et al. 2005). It has been suggested that NLS1 galaxies are less evolved than Seyfert galaxies in that their black holes are still in the process of growing by rapid accretion (e.g., Mathur 2001; Grupe & Mathur 2004; Botte et al. 2004; Mathur & Grupe 2005). Since accretion processes are known to be very efficient in spinning up the accreting black holes (Volonteri et al. 2005 and references therein), one then indeed expects that the final stages, “normal” Seyfert galaxies and quasars, should have on average more rapidly spinning black holes than the NLS1 galaxies.

At the same time, spin cannot be the only quantity making objects radio-loud, or else all quasars would be more radio-loud than NLS1 galaxies. Thus, spin would be a necessary but not sufficient condition. If, indeed, spin plays a role, then the few radio-loud NLS1 galaxies should be those with the more rapidly spinning black holes, already more evolved than others. One may thus expect that they lie closer to the black-hole mass–velocity dispersion ($M_{\text{BH}}-\sigma$) relation of Seyfert galaxies than other NLS1 galaxies. We have plotted the objects of our sample in the $M_{\text{BH}}-\sigma$ plane of Mathur & Grupe (2005, their Fig. 1) and indeed find that they are systematically closer to, or on, the $M_{\text{BH}}-\sigma$ relation followed by Seyfert galaxies.

Future X-ray observations of the iron line may help to search for signs of more rapidly spinning black holes in the radio-loud NLS1 galaxies, but less rapidly spinning black holes in the NLS1 population as a whole.

In summary, while we cannot fully exclude beaming from operating in all sources, the source properties are generally such that this mechanism is not favored (with the three exceptions mentioned above). Accretion mode, possibly in combination with spin, is a possibility.

5.8. Future Work

The results of this study lead us to identify a number of important follow-up observations: High-quality optical spectra of the 11 radio-loudest objects of our sample do not yet exist or are not yet published. Spectra of high resolution and signal-to-noise ratio would allow a search for similarities/differences in emission lines between radio-loud and radio-quiet NLS1 galaxies in the same way it is now rigorously done for broad- and narrow-line objects (e.g., Véron-Cetty et al. 2001; Sulentic et al. 2002; Bachev et al. 2004). Especially important is a reliable decomposition of the faint Balmer lines like $H\gamma$ and $H\delta$ into broad and narrow components and deblending from $[\text{O III}] \lambda 4363$, such that extinction measurements become possible for those objects that have $H\alpha$ redshifted out of the observable optical band. This knowledge is essential for the assessment of radio loudness (in reddened objects, radio loudness is overpredicted) and for black hole mass calculation.

Good optical spectra of the radio-loud and almost radio-quiet NLS1 galaxies, and a comparison sample of quasars, will enable black hole mass and bulge mass estimates using $H\beta$ and $[\text{O III}]$ or low-ionization lines and ideally also absorption features (e.g.,

Grupe & Mathur 2004; Botte et al. 2004; Greene & Ho 2005), which will then allow us to test more rigorously whether claimed systematic trends of higher black hole masses in radio-loud versus radio-quiet quasars extend to the NLS1 population.

X-ray observations of all sources are needed in order to measure accurate spectral shapes, few of them available so far, and to determine the amount of absorption. Deeper X-ray observations are required to measure iron-line profiles in search for (less) rapidly spinning black holes in NLS1 galaxies.

How much of the scatter in radio spectral index of the NLS1 galaxies is real and how much is caused by the nonsimultaneity of the data should be tested with simultaneous radio observations at different frequencies and monitoring for variability. The latter will also constrain the number of beamed sources. Radio observations of higher spatial resolution should be carried out in order to confirm the compactness of the NLS1 galaxies of our sample and thus also to check how far the similarity with known CSS sources goes.

Larger samples of AGNs with a relaxed NLS1 classification criterion where the cut in FWHM is dependent on luminosity will enable us to address the question of whether the fraction of radio-loud NLS1 galaxies systematically changes (increases) with $\text{FWHM}_{H\beta}$ and whether (radio-loud) NLS1 galaxies with higher black hole masses emerge. The largest sample to date of NLS1 galaxies from the SDSS database, but still using an FWHM cut-off, is currently being compiled by Zhou et al. (2005, private communication).

Apart from future multiwavelength follow-up observations of the small sample of radio-loud NLS1 galaxies presented here, Virtual Observatory tools will become more and more important in studying trends throughout the whole NLS1 and AGN populations, since they will allow the extraction of multiwavelength information from existing databases in a homogeneous way, which will then enable us to study the bulk properties of populations on the one hand and to identify exceptional individual sources on the other hand.

6. SUMMARY AND CONCLUSIONS

We have presented a study of the radio properties of NLS1 galaxies, with emphasis on the search for radio-loud NLS1 galaxies. The results of this study can be summarized as follows.

Eleven candidate radio-loud NLS1 galaxies were identified, significantly increasing the number of known radio-loud NLS1 galaxies. These are radio-loud judged on both radio index and radio power. Radio-detected NLS1 galaxies cover several orders of magnitude in radio index R . The distribution is rather smooth below $R \approx 10$.

The fraction of detected radio-loud NLS1 galaxies is $\sim 7\%$, smaller than the fraction of radio-loud galaxies among quasars. Only 2%–3% of the NLS1 galaxies exceed a radio index $R > 100$ (SDSS J172206.03+565451.6, SDSS J094857.3+002225, and possibly the absorbed source TEX 11111+329). This could partly, but likely not fully, be a selection effect arising from the NLS1 definition as objects with $\text{FWHM}_{H\beta} < 2000 \text{ km s}^{-1}$ independent of luminosity.

The radio-loud NLS1 galaxies are generally steep-spectrum sources and compact. Two have inverted spectra. NVSS and FIRST radio fluxes are consistent with each other in most cases, indicating little variability.

Accretion rate estimates show that most sources likely accrete close to or above the Eddington limit. Black hole masses are generally at the upper end observed in NLS1 galaxies [$M_{\text{BH}} \approx (2-10) \times 10^7 M_{\odot}$, for objects with optical spectra of good quality] but still small when compared to some samples of radio-loud

quasars. In particular, the NLS1 galaxies of our sample fill up a previously scarcely populated area of (M_{BH} , R) diagrams.

Optical properties of the radio-loud NLS1 galaxies are similar to those of the NLS1 population as a whole. In particular, their Fe II and [O III] emission covers almost the whole range observed in NLS1 galaxies. Their radio properties, however, extend the range of radio-loud objects to those with small FWHM_{H β} . The fraction of [O III] “blue-wingers” is high. X-ray properties are consistent with the NLS1 population as a whole, with $\Gamma_{\text{sx}} \simeq -2$ to -3.5 and $L_{\text{sx}} \simeq 10^{44}$ – 10^{46} ergs s⁻¹; some sources are highly variable, while others are constant throughout the observation interval.

The starburst contribution to the radio emission, estimated for those sources with *IRAS* 60 μm detections, is small or completely negligible. The AGNs are expected to dominate any starburst in radio emission by factors of 5–115.

We do not find indications for beaming in most of the sources, arguing against the explanation that we see intrinsically radio-quiet but beamed sources. Accretion mode and spin might be factors to account for the lower frequency of radio-loud NLS1 galaxies than radio-loud quasars.

Future studies of radio-loud NLS1 galaxies and follow-up observations of the sample presented here will provide important information on distinguishing between different NLS1 models, on (the existence of) the radio-loud/radio-quiet dichotomy of AGNs, and on accretion disk-jet models.

Note added in manuscript.—While our paper was being refereed, a paper by Whalen et al. (2006) appeared on the astro-ph

preprint server. These authors present optical follow-up spectroscopy of FIRST radio sources identified as NLS1 galaxies, including 16 candidate radio-loud NLS1 galaxies (>50% of their sample have radio power $<10^{24}$ W Hz⁻¹). Their findings are consistent with ours in that both works do not find strong correlations between optical line parameters and radio loudness, and black hole masses show similar ranges. Being a radio-selected sample, the fraction of radio-loud NLS1 galaxies is higher in the sample of Whalen et al.; on the other hand, a number of the sources of Whalen et al. are below a radio power of 10^{24} W Hz⁻¹, and we note that sources significantly above a radio index $R = 1000$ are missing in both studies.

GAVO was funded by the Bundesministerium für Bildung und Forschung under contract 05 AE2EE1/4. D. X. and S. K. acknowledge the support of the Chinese National Science Foundation under grant NSFC-10503005. This work is partially based on a spectrum taken at the Chinese Xinglong 2.16 m telescope. We thank Jiaming Ai for taking the Xinglong spectrum of RX J23149+2243, Hongyan Zhao for sharing part of his observing time with us, and Jian-Min Wang for discussions. We thank Ed Moran for his referee report. This research made use of the SDSS and *ROSAT* archives, the NASA/IPAC Extragalactic Database and VizieR service, and the following catalogs: *IRAS*, USNO-A2, USNO-B1, GSC2.2, FIRST, NVSS, SUMSS, WENSS, PMN, 87GB, PKS, and the Catalogue of Quasars and Active Nuclei.

REFERENCES

- Abazajian, K., et al. 2005, *AJ*, 129, 1755
- Adorf, H.-M., Lemson, G., & Voges, W. 2006, in *ASP Conf. Ser. 351, Astronomical Data Analysis Software and Systems XV*, ed. C. Gabriel et al. (San Francisco: ASP), in press
- Adorf, H.-M., Lemson, G., Voges, W., Enke, H., & Steinmetz, M. 2003, in *ASP Conf. Ser. 314, Astronomical Data Analysis Software and Systems XIII*, ed. F. Ochsenbein, R. Allen, & D. Egret (San Francisco: ASP), 281
- Antonucci, R. 1993, *ARA&A*, 31, 473
- Bachev, R., Marziani, P., Sulentic, J. W., Zamanov, R., Calvani, M., & Dultzin-Hacyan, D. 2004, *ApJ*, 617, 171
- Bade, N., Fink, H. H., Engels, D., Voges, W., Hagen, H.-J., Wisotzki, L., & Reimers, D. 1995, *A&AS*, 110, 469
- Barvainis, R., Lonsdale, C., & Antonucci, R. 1996, *AJ*, 111, 1431
- Bauer, F. E., Condon, J. J., Thuan, T. X., & Broderick, J. J. 2000, *ApJS*, 129, 547
- Becker, R. H., White, R. L., & Helfand, D. J. 1995, *ApJ*, 450, 559
- Beckert, T., & Duschl, W. J. 2002, *A&A*, 387, 422
- Begelman, M. C. 2002, *ApJ*, 568, L97
- Best, P. N., Kauffmann, G., Heckman, T. M., Brinchmann, J., Charlot, S., Ivezić, Z., & White, S. D. M. 2005, *MNRAS*, 362, 25
- Bian, W., & Zhao, Y. 2004, *MNRAS*, 352, 823
- Bicay, M. D., Stepanian, J. A., Chavushyan, V. H., Erastova, L. K., Ayvazyan, V. T., Seal, J., & Kojoian, G. 2000, *A&AS*, 147, 169
- Blandford, R. D. 2000, *R. Soc. London Philos. Trans. A*, 358, 811
- Blandford, R., & Payne, D. G. 1982, *MNRAS*, 199, 883
- Blandford, R., & Znajek, R. L. 1977, *MNRAS*, 179, 433
- Boller, T., Brandt, W. N., & Fink, H. H. 1996, *A&A*, 305, 53
- Boroson, T. A. 2002, *ApJ*, 565, 78
- Boroson, T. A., & Green, R. F. 1992, *ApJS*, 80, 109
- Botte, V., Ciroi, S., Rafanelli, P., & Di Mille, F. 2004, *AJ*, 127, 3168
- Brinkmann, W., Arevalo, P., Gliozzi, M., & Ferrero, E. 2004, *A&A*, 415, 959
- Brinkmann, W., & Siebert, J. 1994, *A&A*, 285, 812
- Celotti, A., & Blandford, R. D. 2001, in *Black Holes in Binaries and Galactic Nuclei*, ed. L. Kaper, E. P. J. van den Heuvel, & P. A. Woudt (New York: Springer), 206
- Cirasuolo, M., Magliocchetti, M., Celotti, A., & Danese, L. 2003, *MNRAS*, 341, 993
- Collin, S., & Kawaguchi, T. 2004, *A&A*, 426, 797
- Condon, J. J., Cotton, D., Greissen, E. W., Yin, Q. F., Perley, R. A., Taylor, G. B., & Broderick, J. J. 1998, *AJ*, 115, 1693
- Czerny, B., Witt, H. J., & Zycki, P. 1997, in *The Transparent Universe*, ed. C. Winkler, T. J.-L. Courvoisier, & P. Drouchoux (Noordwijk: ESA), 397
- de Breuck, C., Tang, Y., de Bruyn, A. G., Rottgering, H., & van Breugel, W. 2002, *A&A*, 394, 59
- Devroye, L., Gyorfi, L., & Lugosi, G. 1996, *A Probabilistic Theory of Pattern Recognition* (Berlin: Springer)
- Elizalde, F., & Steiner, J. E. 1994, *MNRAS*, 268, L47
- Elvis, M. 2000, *ApJ*, 545, 63
- Elvis, M., Plummer, D., Schachter, J., & Fabbiano, G. 1992, *ApJS*, 80, 257
- Elvis, M., et al. 1994, *ApJS*, 95, 1
- Falcke, H., Sherwood, W., & Patnaik, A. R. 1996, *ApJ*, 471, 106
- Falcone, A. D., et al. 2004, *ApJ*, 613, 710
- Fields, D., Mathur, S., Pogge, R., Nicastro, F., Komossa, S., & Krongold, Y. 2005, *ApJ*, 634, 928
- Forster, K., Green, P. J., Aldcroft, T. L., Vestergaard, M., Foltz, C. B., & Hewett, P. C. 2001, *ApJS*, 134, 35
- Gierlinski, M., & Done, D. 2004, *MNRAS*, 349, L7
- Giommi, P., et al. 1991, *ApJ*, 378, 77
- Gliozzi, M., Brinkmann, W., O’Brien, P. T., Reeves, J. N., Pounds, K. A., Trifoglio, M., & Gianotti, F. 2001, *A&A*, 365, L128
- Greene, J. E., & Ho, L. C. 2005, *ApJ*, 627, 721
- Greene, J. E., Ho, L. C., & Ulvestad, J. S. 2006, *ApJ*, 636, 56
- Gregory, P. C., & Condon, J. J. 1991, *ApJS*, 75, 1011
- Griffith, M. R., Wright, A. E., Burke, B. F., & Ekers, R. D. 1994, *ApJS*, 90, 179
- Grupe, D. 2004, *AJ*, 127, 1799
- Grupe, D., Leighly, K. M., Thomas, H.-C., & Laurent-Muehleisen, S. A. 2000, *A&A*, 356, 11
- Grupe, D., & Mathur, S. 2004, *ApJ*, 606, L41
- Grupe, D., Wills, B. J., Leighly, K. M., & Meusinger, H. 2004, *AJ*, 127, 156
- Halpern, J. P., & Moran, E. C. 1998, *ApJ*, 494, 194
- Helfand, D. J., Stone, R. P. S., Wilman, B., White, R. L., Becker, R. H., Price, T., Gregg, M. D., & McMahon, R. G. 2001, *AJ*, 121, 1872
- Hooper, E. J., Impey, C. D., Foltz, C. B., & Hewett, P. C. 1995, *ApJ*, 445, 62
- Hughes, S. A., & Blandford, R. D. 2003, *ApJ*, 585, L101
- Ivezić, Z., et al. 2002, *AJ*, 124, 2364
- Jackson, N., & Browne, I. W. A. 1991, *MNRAS*, 250, 422
- Joly, M. 1991, *A&A*, 242, 49
- Kaspi, S., Maoz, D., Netzer, H., Peterson, B., Vestergaard, M., & Jannuzi, B. T. 2005, *ApJ*, 629, 61
- Kawaguchi, T. 2003, *ApJ*, 593, 69
- Kay, L. E., Magalhaes, A. M., Elizalde, F., & Rodrigues, C. 1999, *ApJ*, 518, 219
- Kellermann, K. I., Sramek, R., Schmidt, M., Shaffer, D. B., & Green, R. 1989, *AJ*, 98, 1195

- Komossa, S., & Mathur, S. 2001, *A&A*, 374, 914
- Komossa, S., & Meerschweinchen, J. 2000, *A&A*, 354, 411
- Komossa, S., Voges, W., Adorf, H.-M., Xu, D., Mathur, S., & Anderson, S. F. 2006, *ApJ*, 639, 710
- Kriss, G. A. 1994, in *ASP Conf. Ser. 61, Astronomical Data Analysis Software and Systems III*, ed. D. R. Crabtree, R. J. Hanisch, & J. Barnes (San Francisco: ASP), 437
- Lacy, M., Laurent-Muehleisen, S. A., Ridgway, S. E., Becker, R. H., & White, R. L. 2001, *ApJ*, 551, L17
- La Franca, F., Gregorini, L., Cristiani, S., de Ruiter, H., & Owen, F. 1994, *AJ*, 108, 1548
- Laor, A. 2000, *ApJ*, 543, L111
- Laor, A., et al. 1997, *ApJ*, 477, 93
- Laurent-Muehleisen, S. A., Kollgaard, R. I., Ryan, P. J., Feigelson, E. D., Brinkmann, W., & Siebert, J. 1997, *A&AS*, 122, 235
- Lawrence, A., Elvis, M., Wilkes, B. J., McHardy, I., & Brandt, W. N. 1997, *MNRAS*, 285, 879
- Leighly, K. 1999, *ApJS*, 125, 297
- Leipski, C., & Bennert, N. 2006, *A&A*, 448, 165
- Lipari, S., Terlevich, R., Diaz, R. J., Taniguchi, Y., Zheng, W., Tsvetanov, Z., Carranza, G., & Dottori, H. 2003, *MNRAS*, 340, 289
- Liu, Y., Jiang, D. R., & Gu, M. F. 2006, *ApJ*, 637, 669
- Maccarone, T. J., Gallo, E., & Fender, R. 2003, *MNRAS*, 345, L19
- Maccarone, T. J., Miller-Jones, J. C. A., Fender, R. P., & Pooley, G. G. 2005, *A&A*, 433, 531
- Madau, P. 1988, *ApJ*, 327, 116
- Mahalanobis, P. C. 1936, *Proc. Natl. Inst. Sci. India*, 2, 49
- Marecki, A., Kunert-Bajraszewska, M., & Spencer, R. E. 2006, *A&A*, 449, 985
- Marziani, P., Sulentic, J. W., Zwitter, T., Dultzin-Hacyan, D., & Calvani, M. 2001, *ApJ*, 558, 553
- Mathur, S. 2000, *MNRAS*, 314, L17
- . 2001, *NewA*, 6, 321
- Mathur, S., & Grupe, D. 2005, *A&A*, 432, 463
- Mauch, T., Murphy, T., Buttery, H. J., Curran, J., Hunstead, R. W., Piestrzynski, B., Robertson, J. G., & Sadler, E. M. 2003, *MNRAS*, 342, 1117
- McLure, R. J., & Jarvis, M. J. 2004, *MNRAS*, 353, L45
- Meier, D. 2003, *NewA Rev.*, 47, 667
- Merritt, D. 2002, *ApJ*, 568, 998
- Metcalfe, R. B., & Magliocchetti, M. 2006, *MNRAS*, 365, 101
- Miller, L., Peacock, J. A., & Mead, A. R. G. 1990, *MNRAS*, 244, 207
- Miller, P., Rawlings, S., & Saunders, R. 1993, *MNRAS*, 263, 425
- Monet, D. G., et al. 2003, *AJ*, 125, 984
- Moran, E. 2000, *NewA Rev.*, 44, 527
- Nagao, T., Murayama, T., Shioya, Y., & Taniguchi, Y. 2002, *ApJ*, 575, 721
- Nagar, N. M., Wilson, A. S., Falcke, H., Veilleux, S., & Maiolino, R. 2003, *A&A*, 409, 115
- Narayan, R., Mahadevan, R., Grindlay, J. E., Popham, R. G., & Gammie, C. 1998, *ApJ*, 492, 554
- O'Brien, P. T., et al. 2001, *A&A*, 365, L122
- Okuda, T., Teresi, V., Toscano, E., & Molteni, D. 2005, *MNRAS*, 357, 295
- Oshlack, A. Y. K. N., Webster, R. L., & Whiting, M. T. 2001, *ApJ*, 558, 578
- . 2002, *ApJ*, 576, 81
- Osterbrock, D. E., & Pogge, R. 1985, *ApJ*, 297, 166
- Padovani, P., Costamante, L., Ghisellini, G., Giommi, P., & Perlmutter, E. 2002, *ApJ*, 581, 895
- Peacock, J. P., & Wall, J. V. 1982, *MNRAS*, 198, 843
- Peterson, B. M., et al. 2000, *ApJ*, 542, 161
- . 2004, *ApJ*, 613, 682
- Pounds, K., Done, C., & Osborne, J. P. 1995, *MNRAS*, 277, L5
- Puchnarewicz, E. M., Mason, K. O., & Cordova, F. A. 1994, *MNRAS*, 270, 663
- Puchnarewicz, E. M., et al. 1992, *MNRAS*, 256, 589
- Remillard, R. A., Bradt, H. V., Buckley, D. A. H., Roberts, W., Schwartz, D. A., Tuohy, I. R., & Wood, K. 1986, *ApJ*, 301, 742
- Remillard, R. A., Grossan, B., Bradt, H. V., Ohashi, T., & Hayashida, K. 1991, *Nature*, 350, 589
- Schlegel, D. J., Finkbeiner, D. P., & Davis, M. 1998, *ApJ*, 500, 525
- Schwoppe, A. D., et al. 2000, *Astron. Nachr.*, 321, 1
- Shemmer, O., & Netzer, H. 2002, *ApJ*, 567, L19
- Shemmer, O., Netzer, H., Maiolino, R., Oliva, E., Croom, S., Corbett, E., & di Fabrizio, L. 2004, *ApJ*, 614, 547
- Shields, G., Gebhardt, K., Salviander, S., Wills, B. J., Xie, B., Brotherton, M. S., Yuan, J., & Dietrich, M. 2003, *ApJ*, 583, 124
- Siebert, J., Leighly, K. M., Laurent-Muehleisen, S. A., Brinkmann, W., Boller, Th., & Matsuoka, M. 1999, *A&A*, 348, 678
- Simkin, M. V., & Roychowdhury, V. P. 2003, *Complex Systems*, 14, 269
- Smith, D. A., Herter, T., & Haynes, M. P. 1998, *ApJ*, 494, 150
- Smith, J. E., Robinson, A., Young, S., Axon, D. J., & Corbett, E. A. 2005, *MNRAS*, 359, 846
- Stepanian, J. A., et al. 2003, *ApJ*, 588, 746
- Sulentic, J. W., Marziani, P., Zamanov, R., Bachev, R., Calvani, M., & Dultzin-Hacyan, D. 2002, *ApJ*, 566, L71
- Sulentic, J. W., Zamfir, S., Marziani, P., Bachev, R., Calvani, M., & Dultzin-Hacyan, D. 2003, *ApJ*, 597, L17
- Ulvestad, J. S., Antonucci, R. R. J., & Goodrich, R. W. 1995, *AJ*, 109, 81
- Urry, C. M., & Padovani, P. 1995, *PASP*, 107, 803
- Vanden Berk, D. E., et al. 2001, *AJ*, 122, 549
- Vaughan, S., Reeves, J., Warwick, R., & Edelson, R. 1999, *MNRAS*, 309, 113
- Véron-Cetty, M.-P., & Véron, P. 2003, *A&A*, 412, 399 (VQC03)
- Véron-Cetty, M.-P., Véron, P., & Gonçalves, A. C. 2001, *A&A*, 372, 730
- Vestergaard, M., Wilkes, B. J., & Barthel, P. D. 2000, *ApJ*, 538, L103
- Visnovsky, K. L., Impey, C. D., Foltz, C. B., Hewett, P. C., Weymann, R. J., & Morris, S. L. 1992, *ApJ*, 391, 560
- Voges, W., et al. 1999, *A&A*, 349, 389
- Volonteri, M., Madau, P., Quataert, E., & Rees, M. J. 2005, *ApJ*, 620, 69
- Wandel, A., Peterson, B. M., & Malkan, M. A. 1999, *ApJ*, 526, 579
- Wang, J.-M., Ho, L. C., & Staubert, R. 2003, *A&A*, 409, 887
- Wang, J.-M., & Netzer, H. 2003, *A&A*, 398, 927
- Wang, J., Wei, J.-Y., & He, X.-T. 2004, *Chinese J. Astron. Astrophys.*, 4, 415
- Wang, T. G., Brinkmann, W., & Bergeron, J. 1996, *A&A*, 309, 81
- Wang, T. G., Matsuoka, M., Kubo, H., Mihara, T., & Negoro, H. 2001, *ApJ*, 554, 233
- Warner, C., Hamann, F., & Dietrich, M. 2004, *ApJ*, 608, 136
- Wei, J. Y., Xu, D. W., Cao, L., Zhao, Y.-H., Hu, J.-Y., & Li, Q.-B. 1998, *A&A*, 329, 511
- Whalen, D. J., Laurent-Muehleisen, S. A., Moran, E. C., & Becker, R. H. 2006, preprint (astro-ph/0601162)
- Whalen, J., Laurent-Muehleisen, S. A., Moran, E. C., & Becker, R. H. 2001, *BAAS*, 33, 1373
- White, R. L., Becker, R. H., Helfand, D. J., & Gregg, M. D. 1997, *ApJ*, 475, 479
- White, R. L., et al. 2000, *ApJS*, 126, 133
- Wills, B., Shang, Z., & Yuan, J. M. 2000, *NewA Rev.*, 44, 511
- Wilson, A. S., & Colbert, E. J. M. 1995, *ApJ*, 438, 62
- Woo, J.-H., & Urry, M. C. 2002, *ApJ*, 579, 530
- Xu, D. W., Komossa, S., Wei, J. Y., Qian, Y., & Zheng, X. Z. 2003, *ApJ*, 590, 73
- Xu, D., et al. 2006, *ApJ*, submitted
- Ye, Y.-C., & Wang, D.-X. 2005, *MNRAS*, 357, 1155
- Yi, I., & Boughn, S. P. 1998, *ApJ*, 499, 198
- York, D. G., et al. 2000, *AJ*, 120, 1579
- Yun, M. S., Reddy, N. A., & Condon, J. J. 2001, *ApJ*, 554, 803
- Zdziarski, A. A., Lubiński, P., Gilfanov, M., & Revnivtsev, M. 2003, *MNRAS*, 342, 355
- Zheng, X. Z., Xia, X. Y., Mao, S., Wu, H., & Deng, Z. G. 2002, *AJ*, 124, 18
- Zheng, Z., Wu, H., Mao, S., Xia, X.-Y., Deng, Z.-G., & Zou, Z.-L. 1999, *A&A*, 349, 735
- Zhou, H.-Y., Wang, T.-G., Dong, X.-B., Zhou, Y.-Y., & Li, C. 2003, *ApJ*, 584, 147
- Zhou, H.-Y., Wang, T.-G., Zhou, Y.-Y., Li, C., & Dong, X.-B. 2002, *ApJ*, 581, 96